

Energy Minimization of Inland Waterway USVs for IRS-Assisted Hybrid UAV-Terrestrial MEC Network

Yangzhe Liao, Jiaying Liu, Xiyu Chen, Yi Han, Qingsong Ai and Gabriel-Miro Muntean, *IEEE Fellow*

Abstract—Due to its exceptional ability to create favorable line-of-sight (LoS) propagation environments, the intelligent reflecting surface (IRS) is widely recognized as a technological enabler for wireless inland waterway communications. In this paper, an IRS-assisted hybrid unmanned aerial vehicles (UAV)-terrestrial network architecture with unmanned surface vehicles (USVs) is proposed and a USVs energy minimization problem is formulated by jointly considering offloading decisions, computation capability, beamforming vector design and IRS phase shift-vector. To address the formulated problem, we decouple the original problem into two subproblems, in which the first subproblem focuses on joint offloading decisions and computation capability and the second subproblem concerns joint IRS phase shift-vector and the beamforming vector design. The enhanced differential evolution algorithm (EDE) is proposed to solve the former subproblem, and the minimum-variance-distortionless-response (MVDR) and enhanced min-maximization (EMM) algorithms are proposed to obtain optimized beamforming vector and IRS phase shift-vector in the second subproblem, respectively. Simulation results show how the proposed solution realizes a good tradeoff between network energy consumption and capacity in comparison to three alternative algorithms. The results also show that the proposed algorithm can improve the network performance in terms of the number of successfully offloaded tasks.

Index Terms—Wireless Inland Waterway Communications, Intelligent Reflecting Surface, Unmanned Aerial Vehicles, Mobile Edge Computing, Quality of Service.

I. INTRODUCTION

A. Background and Motivation

WITH the increasing popularity of low-cost and fully autonomous unmanned surface vehicles (USVs) and rapid deployment of the fifth-generation (5G) communications infrastructure, both academia and industry have been enthusiastic regarding research in the field of wireless inland waterways communications [1-3]. Currently, USVs can generate a large amount of data that needs to be processed in real-time, such as marine resource exploration, environmental monitoring, maritime search and rescue, autonomous navigation and so forth. However, USVs are commonly operated far away from the energy source and must be powered by onboard batteries with limited computational capabilities and suffering substantial technical challenges to satisfy the strict quality of service

Y. Liao, J. Liu, X. Chen, Y. Han are with the School of Information Engineering, Wuhan University of Technology, Wuhan, 430070, China

Q. Ai is with the School of Computer Science and Information Engineering, Hubei University, Wuhan, China, 430062 & Wuhan University of Technology

Gabriel-Miro Muntean is with the School of Electronic Engineering, Dublin City University, Ireland

This work was supported in part by the Natural Science Foundation of China under Grant 52201417. The work of Prof. Muntean was supported by the Science Foundation Ireland via grant 12/RC/2289_P2 (INSIGHT). (Corresponding author: Yi Han)

(QoS) requirements of their resource-intensive tasks [4-5]. Moreover, due to the unpredictable and randomness of wireless communication channels between USVs and terrestrial base stations (TBSs), signal transmission suffers reflections, diffractions and scattering, resulting in attenuation and delay [6-9]. Such channel effects become critical negative factors in the quest to enhance wireless inland waterways communications performance, including network energy efficiency.

Mobile/multi-access edge computing (MEC) is a novel communication approach in the 5G era, bringing cloud-like computing resources to the network edge, specifically to TBSs [10-13]. In particular, MEC is capable of improving the computation capability of USVs by allowing them to offload computation-intensive and latency-sensitive tasks to resource-rich MEC servers. In this manner, the majority of task execution-related energy consumption can be transferred from battery-limited USVs to MEC servers. Although applying tethered unmanned aerial vehicles (UAVs) to inland waterway environments can offer UAVs substantial additional energy supply to serve data transmission and processing, it is still a challenge to design efficient offloading solutions. Particularly it is challenging to enable the use of MEC server computation capabilities to support USVs' communication and computation cooperation when tasks cannot be successfully offloaded due to poor transmission link quality [14]. An additional issue when realizing a sustainable UAV-based MEC network is related to the limitation in terms of the energy supply.

In the last period, one commonly used approach for mobile network operators to handle data transmission problems has been to deploy more TBSs. However, this method suffers from large energy waste, severe interference and especially huge operational costs. Fortunately, with the rapid progress in meta-materials, an innovative sixth-generation (6G) technology, namely intelligent reflecting surface (IRS), has been introduced in the wireless communication community as a promising solution to establish an intelligence propagation environment [15]. As a revolutionary technique in non-terrestrial wireless communications, IRS-assisted UAV MEC systems are expected to offer support in terms of low energy consumptions, short transmission delays, simple hardware implementations, extended flight durations and so on. Unfortunately, currently this emerging technology is affected by significant limitations in relation to the acquisition of accurate channel state information (CSI) at the IRS.

B. The Main Contributions

According to the above background and technical difficulties, deploying a UAV to perform as a relay in the air to

serve USVs in inland waterway environments or deploying an IRS near TBS requires mobile network operators to install new telecommunications infrastructure, which is both expensive and time-consuming. One effective way to improve the energy efficiency of the network performance is to utilize a UAV-mounted IRS-assisted MEC network over an aerial relay network, in conjunction with the existing communication network. The resource allocation schemes for USVs' energy minimization in IRS-assisted hybrid UAV-terrestrial MEC network are of great significance in overcoming the battery and computation capability limitations of USVs. Although some resource allocation schemes were designed for energy efficiency optimization in IRS-assisted MEC networks, there are very few works to address the resource allocation schemes for energy efficiency of USVs in IRS-assisted hybrid UAV-terrestrial networks because of the challenging optimization. In particular, an energy-efficient joint resource allocation of USVs' energy consumption in IRS-assisted hybrid UAV-terrestrial MEC networks is not yet available in the literature. Motivated by the reasons above, the energy minimization problem of USVs by jointly considering USVs' offloading decisions, USVs' computation capabilities, beamforming vector, and IRS shift-vector is formulated. A heuristic solution is proposed to realize the corresponding resource allocations and obtain the suboptimal solution to the challenging formulated problem. With this solution, superior energy efficiency performance is achieved. The main contributions of this paper are listed as follows

- 1) The tethered UAV-mounted IRS brings numerous technical advantages. First, tethered UAV can obtain a reliable energy supply by TBS via cable to support heavy load capacity to carry large-area IRS. In this way, the frequency of information exchange between TBS and IRS can be significantly decreased, USVs can offload computation tasks to TBS for execution with the assistance of UAV-mounted IRS and enjoy reliable wireless link quality. Moreover, the design of TBS beamforming vector to serve each USV and IRS phase shift-vector only relies on the statistical CSI obtained from location information, which varies considerably slower compared with the instantaneous CSI and the shared data size of location information between TBS and IRS controller is extremely small that can be neglected. In addition, each IRS is connected to an IRS controller, which is able to adjust the amplitude and phase of incident signals from USVs. Consider the technical advantages of tethered UAV-mounted IRS-assisted transmission, a novel IRS-assisted hybrid UAV-terrestrial MEC network architecture with USVs is proposed, where each USV can offload its computation task to MEC server directly or assisted by a tethered UAV-mounted IRS.
- 2) Aiming to prolong USVs' network lifetime, this paper formulates USVs' energy minimization by jointly considering USVs' offloading decisions, USVs' computation capability, beamforming vector design and IRS phase shift-vector. To address the formulated problem, a heuristic solution called DMM is proposed. The solution involves

dividing the challenging original optimization problem into two subproblems and solving them with novel algorithms. First, the joint USVs offloading decisions and computation capability subproblem is solved using a proposed enhanced differential evolution algorithm (EDE). Then, by employing the solution to this subproblem, the second subproblem is focused on obtaining the optimal beamforming vector and IRS phase shift-vector. The paper introduces the minimum variance distortionless response algorithm (MVDR) and the enhanced minimaximization algorithm (EMM), which are used in an iterative manner, respectively.

- 3) The proposed solution improves the system performance, especially in terms of energy consumption. The results verify that the proposed algorithms considerably decrease USVs' energy consumption in comparison with a wide range of alternative energy-efficient algorithms. Moreover, the results also demonstrate that the network capacity can be significantly enhanced by utilizing the proposed IRS-based DMM.

The rest of the paper is organized as follows. The system model and the formulated optimization problem are given in Section II. The proposed heuristic solution is introduced in Section III. The performance evaluation of the proposed solution is compared with that of some selected advanced algorithms in Section IV. Finally, conclusions are drawn in Section V.

II. RELATED WORKS

A. UAV-Enabled MEC Networks

Ren *et al.* proposed a joint resource allocation and task offloading strategy to enhance the QoS of mobile devices [16]. The results showed that the network energy consumption could be remarkably reduced while satisfying average execution latency requirements. However, this technique only focused on a single-user case and cannot be applied to a multi-user network. The authors of [17] mentioned that a major technical difficulty in the event of task offloading scheduling is determining offloading decisions since mobile devices may suffer an amount of transmission energy consumption to offload tasks to MEC server, and consequently for the receiving of computation results from MEC server. The authors of [18] demonstrated that each mobile device offloading decision could affect other devices offloading decisions; some mobile devices may even increase their transmission power to obtain high link quality, leading to severe interference and increasing the transmission failure probability. Wang *et al.* proposed that mobile devices can be divided into different sets, e.g., local execution set, offloading set and reschedule set, based on data size, latency requirement, network interference and the remaining computation resource of MEC server. Mobile devices from the offloading set are allowed to offload tasks to MEC server while devices in the local execution set and reschedule set can only be locally executed. In this way, the number of successfully offloaded tasks can be increased. The authors of [19] proposed an UAV-enabled MEC network architecture by integrating UAVs with a MEC server. The

results showed that this emerging network architecture could serve mobile devices in a more flexible manner compared with terrestrial MEC networks. The authors of [20] investigated the energy minimization problem of the proposed UAV-empowered MEC network by jointly considering mobile devices offloading decisions, network resource allocation and UAV trajectory. To address the formulated challenging problem, the authors first divided the original problem into two subproblems and then utilized an alternating optimization algorithm to solve each subproblem iteratively. Fortunately, tethered UAVs bring a novel solution to this technical difficulty. In particular, each tethered UAV is capable of receiving a stable energy supply via a tether connected to TBS and offering durable communication and computation services in places lacking telecommunications infrastructure. In this way, the main design challenges of an untethered UAV-enabled MEC system, e.g., UAV's energy minimization, can be successfully solved by deploying tethered UAV. AT&T utilized a low-altitude tethered UAV at around 60 meters to provide temporary communication service in Puerto Rico after Hurricane Maria in 2017 [21]. The author of [22] proposed a tethered UAV-assisted MEC system to serve a list of mobile users. The results validated the effectiveness of tethered UAV in enhancing task offloading energy efficiency performance. The authors of [23] designed an energy-efficient task scheduling framework for a tethered UAV-based MEC network in rural areas. The results showed that by utilizing sufficient energy supplied tethered UAVs, the network could successfully execute a higher number of offloaded tasks.

B. IRS-assisted Wireless Communications

IRS is a two-dimensional meta-surface consisting of an array of passive/active scattering electromagnetic elements and each element can be controlled to change the electromagnetic properties, including incident signal phase shift and reflection angle to realize various purposes, such as beam-steering, beam-splitting, diffusion and polarization [24]. Note that IRS may serve multiple communicating entities simultaneously by splitting the incident beam into sub-beams and adjusting each sub-beam to focus on one specific direction; this technology suffers extremely technical difficulties, such as the hybrid beamforming design of TBS and the active beamforming design of IRS. As such, the majority of the current research works focus on IRS to perform the beam focusing function on serving one communicating entity. Zhang *et al.* proposed that IRS technology can be used to create smart signal prorogation environments and support imperfect phase compensation for severe signal transmission attenuation [25]. Different from the traditional amplify-and-forward (AF) and decode-and-forward (DF) relaying techniques that consume substantial energy to receive and process the received signal, IRS has an extremely low energy consumption and each element is able to coordinate the dynamic wireless environments. The authors of [26] investigated the comparative performance between the AF relaying technique and IRS-assisted data transmission. The results showed that IRS realizes higher energy efficiency than the DF relaying under high rates scenarios. Moreover, the lightweight IRS realizes satisfactory compatibility for

flexible deployments. For example, IRS can be either coated on terrestrial objects such as walls or installed on different types of existing aerial platforms, such as UAVs and satellites, without installing any new hardware.

C. IRS-assisted UAV MEC Systems and CSI Acquisition

Wang *et al.* investigated the energy minimization problem by jointly considering the beamforming vector and IRS phase shift-vector design for IRS-assisted UAV networks [27]. Moreover, the authors assumed that each time slot is sufficiently long to allow each mobile device to offload tasks, adjust computation capability and complete task execution. The authors of [28] formulated the latency minimization problem for IRS-assisted UAV MEC networks by jointly considering passive IRS phase shift-vector and mobile devices' offloading schedules. However, this approach only considered a two-user case and cannot be applied to real world scenarios. Wu *et al.* demonstrated that the network sum-rate could be significantly improved by joint optimizing IRS beamforming gain and UAV trajectory [29]. The results showed that the integration of IRS and UAV could considerably enhance the non-terrestrial network performance in terms of energy consumption and UAV trajectory can be more flexible. The authors of [30] proposed an IRS-assisted UAV MEC network architecture, where a UAV is used to create a line-of-sight (LoS) link between UAV and ground mobile devices. The results showed that the network energy efficiency could be effectively improved. Aiming to minimize UAV swarm energy consumption, the authors of [31] presented a four-phase-based algorithm to jointly optimize UAV swarm trajectories and IRS phase shift-vector in a novel multi-IRS and multi-UAV-assisted MEC network architecture. The authors of [32] proposed a unified dynamic beamforming framework to boost the energy efficiency of an IRS-assisted MEC network. The results showed that the computational mode selection of mobile devices and IRS beamforming design are highly coupled. Under the assumption that task offloading is with the assistance of IRS in both flat-fading and frequency-selective channels, Sun *et al.* proposed that the mobile devices energy minimization problem for an IRS-assisted MEC network is considered by jointly optimizing their local CPU frequencies, offloading decisions, task size and IRS phase shift-vector [33]. Some perspective scenarios regarding energy efficiency enhancement of IRS-assisted UAV-enabled MEC networks are described in [34]. Although some resource allocation schemes were designed for energy efficiency optimization in IRS-assisted MEC network, there are very few works to address the resource allocation schemes for energy efficiency of USVs in IRS-assisted hybrid UAV-terrestrial networks because of the challenging optimization.

The authors of [35] investigated the channel estimation problem and compared the energy efficiency performance between passive IRS and hybrid IRS systems. The results show that CSI of purely passive IRS scenarios can be easily obtained, which is of significant importance to shift the fundamental paradigm of wireless network design in the real world. The authors of [36] reported that the statistical CSI acquisition could be realized by using the location information-aided scheme with reduced overhead of channel estimation

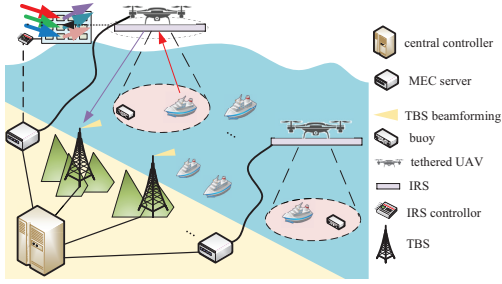


Fig. 1: The proposed IRS-assisted hybrid UAV-terrestrial network architecture with USVs.

for a reflecting-only IRS-assisted network in comparison with instantaneous CSI. As a result, the reflecting-only IRS-assisted transmission methods are widely recognized as a promising technology for creating smart wireless communication environments with low hardware implementation complexity with the statistical CSI. The authors of [37] proposed that CSI for a fully passive IRS-assisted UAV-enabled system can be effectively estimated based on the received pilot signals from the transmitter or receiver by designing IRS phase shift-vector and then the obtained CSI can be wirelessly transmitted to IRS controller to adjust IRS phase shift-vector. The authors of [38] explored the relationship between IRS phase shift design, the number of required IRS reflecting elements and UAV flight time. The results showed that UAV flight time could be remarkably prolonged by decreasing the number of IRS reflecting elements. Note that tethered UAV-mounted IRS can receive a reliable energy supply in practice, offering extremely long-endurance operations. In addition, tethered UAVs can support heavy load capacity to carry large-area IRS to support diverse functionalities, such as offering full 360-degree angle reflection toward the ground and assisting wireless transmission between any pair of communicating entities with LoS channels.

III. SYSTEM MODEL AND PROBLEM FORMULATION

Fig. 1 shows the proposed IRS-assisted hybrid UAV-terrestrial MEC network architecture with USVs. In this system, a set of tethered J UAVs, denoted as $\mathcal{J} = \{1, 2, \dots, J\}$, are dynamically dispatched and form virtual clusters with TBSs to serve a set of N single-antenna USVs, denoted as $\mathcal{N} = \{1, 2, \dots, N\}$. Each tethered UAV is equipped with a K -element IRS¹ and the phase shift-vector is denoted by $\boldsymbol{\theta} = [\theta_1, \theta_2, \dots, \theta_K]^T$ with $\theta_k \in [0, 2\pi), k \in [1, 2, \dots, K]$. Moreover, each MEC server is placed next to a M -antenna TBS via optical fiber and is utilized to perform computation services and deliver power supplies for tethered UAVs. In the same manner with [39], UAV-mounted IRS transmission links are assumed based on long-term statistical CSI to reduce the signaling and hardware implementation complexity. In addition, we assume that MEC server is aware of the locations of UAVs and CSI² as a *priori*.

¹In this paper, IRS element spacing is assumed sufficient enough and thus we ignore the small-scale fading associated with any two reflecting elements.

²In this paper, the statistical CSI can be effectively obtained using the location information aided method proposed in [40].

Assume that during each equal-length time slot, each USV i randomly generates a computation task, denoted by $U_i = (D_i, F_i, T_i), i \in \mathcal{N}$. D_i , F_i and T_i denote the task size (in bits), the number of required CPU cycles and the maximum time allowance to execute task U_i , respectively. Moreover, each task U_i is assumed as indivisible and can either be locally executed by USV i itself or offloaded to a MEC server for execution. Similar to [27], each time slot is assumed sufficiently long to enable each USV to offload tasks, adjust computation capability and complete task execution. Note that each tethered UAV is assumed to fly at the fixed height H and can simultaneously serve no more than one USV.

A. Network Computation and Communication Models

Considering each virtual cluster, denote α_i as the offloading indicator of USV i , where $\alpha_i = 1$ means that USV i decides to offload task U_i while $\alpha_i = 0$ means otherwise. When USV i decides to execute task by itself, i.e., $\alpha_i = 0$, the local execution time can be expressed as:

$$T_i^l = \frac{F_i}{f_i}, i \in \mathcal{N}, \quad (1)$$

where f_i is the computation capability of USV i . The corresponding energy consumption of USV i can be expressed as:

$$E_i^l = T_i^l \kappa_i (f_i)^{\zeta_i}, i \in \mathcal{N}, \quad (2)$$

where κ_i and ζ_i are the switched capacitance and positive constant, respectively, which are both dependent on USV i 's hardware architecture.

The amplitude reflection coefficient is defined as β , which ranges from $[0, 1]$ and thus IRS reflection-coefficient matrix can be expressed as:

$$\boldsymbol{\Theta} = \text{diag}(\beta e^{j\theta_1}, \beta e^{j\theta_2}, \dots, \beta e^{j\theta_K}). \quad (3)$$

Similar to [41], we assume that IRS follows a full reflection, and thus the value of β is set to 1. Let p_i^{tr} and s_i be the transmission power and unit-power signal of USV i , respectively. Define $\mathbf{n} \sim \mathcal{CN}(0, \sigma^2 \mathbf{I})$ as the noise with mean zero and variance $\sigma^2 \mathbf{I}$. When USV i decides to offload its task with the assistance of IRS, i.e., $\alpha_i = 1$, the received signal at TBS from USVs via IRS-assisted offloading can be given as:

$$\mathbf{y} = \sum_{i=1}^N \sqrt{p_i^{tr}} (\mathbf{h}_{d,i} + \mathbf{G}\boldsymbol{\Theta}\mathbf{h}_{r,i}) s_i + \mathbf{n}, \quad (4)$$

where $\mathbf{h}_{d,i} \in \mathbb{C}^{M \times 1}$, $\mathbf{h}_{r,i} \in \mathbb{C}^{K \times 1}$ and $\mathbf{G} \in \mathbb{C}^{M \times K}$ are the channel gain from USV i to TBS, USV i to IRS and IRS to TBS, respectively. Since the signal transmitted from USV i is processed by TBS with the multi-user detection technique and thus one has $y_i = \mathbf{w}_i^H \mathbf{y}$, where $\mathbf{w}_i \in \mathbb{C}^{M \times 1}$ is the beamforming vector of TBS to serve each USV i , the corresponding signal to interference noise ratio (SINR) at TBS can be expressed as:

$$\gamma_i = \frac{p_i^{tr} \|\mathbf{w}_i^H (\mathbf{h}_{d,i} + \mathbf{G}\boldsymbol{\Theta}\mathbf{h}_{r,i})\|^2}{\sum_{j \neq i}^N p_j^{tr} \|\mathbf{w}_i^H (\mathbf{h}_{d,j} + \mathbf{G}\boldsymbol{\Theta}\mathbf{h}_{r,j})\|^2 + \sigma^2 \|\mathbf{w}_i\|^2}, \quad (5)$$

$i, j \in \mathcal{N}, i \neq j,$

where $\mathbf{h}_{d,j} \in \mathbb{C}^{M \times 1}$ is the channel gain from USV j to the corresponding TBS.

The corresponding IRS-assisted offloading channel capacity can be given as:

$$C_i = B_i \log_2(1 + \gamma_i), i \in \mathcal{N}, \quad (6)$$

where B_i is the allocated bandwidth of USV i .

The corresponding transmission time from USV i to MEC server can be expressed as:

$$T_i^{tr} = \frac{D_i}{C_i}, i \in \mathcal{N}. \quad (7)$$

Finally, the corresponding offloading energy consumption of USV i is:

$$E_i^{tr} = p_i^{tr} T_i^{tr}, i \in \mathcal{N}. \quad (8)$$

B. Problem Formulation

In this paper, we aim to prolong the network lifetime of battery empowered USVs, that is, to minimize the energy consumption of USVs by jointly considering USVs' offloading decisions $\alpha = \{\alpha_i, i \in \mathcal{N}\}$, USVs' computation capabilities $\mathbf{f} = \{f_i, i \in \mathcal{N}\}$, beamforming vector \mathbf{w}_i and IRS phase shift-vector θ , which can be formulated as:

$$\begin{aligned} \mathcal{P}1: \quad & \min_{\alpha, \mathbf{f}, \theta, \mathbf{w}_i} E^{total} = \sum_{i=1}^N ((1 - \alpha_i) E_i^l(f_i) + \alpha_i E_i^{tr}(\theta, \mathbf{w}_i)) \\ \text{s.t.} \quad & \mathcal{C}1: \alpha_i \in \{0, 1\}, i \in \mathcal{N}, \\ & \mathcal{C}2: f_i^{min} \leq f_i \leq f_i^{max}, i \in \mathcal{N}, \\ & \mathcal{C}3: 0 \leq \theta_k < 2\pi, k = 1, 2, \dots, K. \end{aligned} \quad (9)$$

Constraint $\mathcal{C}1$ points out that the offloading decision variable of each USV i is a 0-1 binary integer. Note that when each USV decides to offload a task, USV can offload this task to MEC server directly or assisted by a UAV-mounted IRS, where the offload decision of each USV can be determined whether to be locally executed or offloaded, regardless of the specific content of task and the practice of ignoring the specific information of offloading task in this paper follows the recent literature [42-44]. Constraint $\mathcal{C}2$ indicates that the computation capability of USV i should follow the range of $[f_i^{min}, f_i^{max}]$, where f_i^{min} and f_i^{max} denote the minimum and maximum allocated computation resources of each USV i for task execution, respectively. Constraint $\mathcal{C}3$ specifies that phase shift of each IRS element k ranges within $[0, 2\pi)$. Note that in the studied IRS-assisted hybrid UAV-terrestrial network, USVs are assumed to follow the same range of computation capability, i.e., $[f_i^{min}, f_i^{max}]$.

Note: $\mathcal{P}1$ is a non-linear non-convex optimization problem, which is challenging to be solved, due to the following aspects. First, due to Constraint $\mathcal{C}1$, the existing exhaustive searching approaches cannot be efficient to solve $\mathcal{P}1$ even with extremely high time costs and computation resources. Moreover, one can observe that optimization variables are closely coupled, resulting in extremely high dimensional variables with the expansion of network size. Consider computation offloading problems of USVs, due to the close couplings among different USVs, channel conditions, the energy status and computation

capability of USVs, it is generally challenging to optimize the offloading decision strategy. The research on this type of optimization problem has not been comprehensively investigated and only a few works are available, such as [14]. Inspired by [45], DE algorithm is proposed as a simple and efficient algorithm to solve global optimization problems. However, the DE algorithm cannot effectively solve large-scale optimization problems. For example, in the studied network, when each USV generates 20 tasks during each time slot, this involves $10 \times 20 \times (2 + K + M)$ optimization variables when $N = 10$. As such, DE may become inefficient in solving the formulated optimization problem $\mathcal{P}1$, even when using large amounts of computation resources.

IV. DMM - THE PROPOSED HEURISTIC SOLUTION

In this section, DMM, a heuristic solution is proposed to solve the challenging formulated problem $\mathcal{P}1$. In particular, we first decouple $\mathcal{P}1$ into two subproblems, i.e., the joint optimization subproblem of α and \mathbf{f} and the joint optimization subproblem of θ and \mathbf{w}_i . The EDE algorithm is proposed to tackle the first subproblem and obtain the feasible solutions of α and \mathbf{f} . Then, by substituting the obtained feasible α and \mathbf{f} into the latter subproblem, the optimal beamforming vector and IRS phase shift-vector can be obtained via utilizing MVDR algorithm and the EMM algorithm, respectively, in an iterative manner. In this way, one can solve the challenging formulated problem $\mathcal{P}1$ efficiently.

A. The Joint Optimization Problem of α and \mathbf{f}

Given any feasible θ and \mathbf{w} , $\mathcal{P}1$ can be reduced to:

$$\begin{aligned} \mathcal{P}1.1: \quad & \min_{\alpha, \mathbf{f}} \sum_{i=1}^N ((1 - \alpha_i) F_i \kappa_i(f_i)^{\zeta_i - 1} + \alpha_i E_i^{tr}) \\ \text{s.t.} \quad & \mathcal{C}1 - \mathcal{C}2. \end{aligned} \quad (10)$$

Note that it is still challenging to solve $\mathcal{P}1.1$ due to the existence of constraint $\mathcal{C}1$. As an efficient global optimization and heuristic search algorithm, DE has been widely used to solve a number of optimization problems, such as big data optimization, order scheduling and so forth. In comparison with other evolutionary algorithms, DE has a strong convergence ability and robustness [46]. In this paper, an enhanced DE algorithm (EDE) is proposed to solve $\mathcal{P}1.1$, where the significant steps, e.g., encoding, mutation, crossover, analysis of boundary condition and offspring selection, are given in detail as follows.

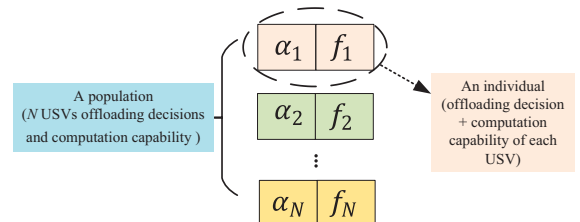


Fig. 2: The proposed encoding mechanism.

Encoding: The proposed encoding mechanism is demonstrated in Fig. 2, where each individual can be regarded as a joint offloading decision and computation capability allocation of each USV. Let $\mathbf{p}_i^g = (\boldsymbol{\alpha}_i, \mathbf{f}_i)^g, i \in \mathcal{N}$ be the population in the g -th generation of USV i , where each population can be expressed as $(\boldsymbol{\alpha}_i, \mathbf{f}_i)^g = ((\alpha_i, f_i)_1^g, (\alpha_i, f_i)_2^g, \dots, (\alpha_i, f_i)_N^g)$. In this way, the length of each individual can be reduced from $N \times 2N$ to $2 \times N$ in comparison with the traditional DE algorithm [47]. At the initialization stage, the initial generation individual can be expressed as:

$$(\boldsymbol{\alpha}_i, \mathbf{f}_i)^0 = (\boldsymbol{\alpha}^L, \mathbf{f}^L) + [\boldsymbol{\rho} \cdot \{(\boldsymbol{\alpha}^U, \mathbf{f}^U) - (\boldsymbol{\alpha}^L, \mathbf{f}^L)\}], i \in \mathcal{N}, \quad (11)$$

where $\boldsymbol{\rho} \in \mathbb{C}^{1 \times 2}$ and each element of $\boldsymbol{\rho}$ is a random number uniformly distributed between 0 and 1. $\boldsymbol{\alpha}^U, \boldsymbol{\alpha}^L, \mathbf{f}^U, \mathbf{f}^L$ represent the upper and the lower bound of $\boldsymbol{\alpha}, \mathbf{f}$, respectively.

Mutation: The individual variation can be realized by employing the differential strategy. As recommended in [48], a common differential strategy DE/rand/1 is selected and utilized. Let the g -th generation mutation vector be $(\boldsymbol{\nu}_i, \mathbf{u}_i)^g = ((\nu_i, u_i)_1^g, (\nu_i, u_i)_2^g, \dots, (\nu_i, u_i)_N^g), i \in \mathcal{N}$, one has:

$$\begin{aligned} (\nu_i, u_i)_n^g &= (\alpha_i, f_i)_{r_1}^g + F \cdot ((\alpha_i, f_i)_{r_2}^g - (\alpha_i, f_i)_{r_3}^g) \\ &= (\alpha_i, f_i)_{r_1}^g + (\text{int}[F \cdot ((\alpha_i)_{r_2}^g - (\alpha_i)_{r_3}^g)], \\ &F \cdot ((f_i)_{r_2}^g - (f_i)_{r_3}^g)), n \neq r_1 \neq r_2 \neq r_3, \end{aligned} \quad (12)$$

where $F \in [0, 2]$ is the mutation operator. The operator $\text{int}[\cdot]$ indicates to obtain the nearest integer number. Let g_{max} be the maximum number of generations. For simplicity, g_{max} is also utilized to represent the predetermined maximum number of iterations of the proposed EDE algorithm. The adaptive mutation operator is proposed to prevent premature convergence, which can be expressed as:

$$F = F_0 \cdot 2^{e^{-\frac{g_{max}}{g_{max}+1-g}}}, \quad (13)$$

where F_0 is the mutation operator and F ranges from $[F_0, 2F_0]$. To maintain individual diversity and avoid premature convergence, F gradually decreases and finally approaches F_0 . In this respect, adaptive mutation can enhance the network performance regarding the probability of finding feasible solutions.

Crossover: To increase the diversity, crossover operation is conducted on each pair of g -th generation individual $(\boldsymbol{\alpha}_i, \mathbf{f}_i)^g$ and mutation individual $(\boldsymbol{\nu}_i, \mathbf{u}_i)^g$. One can obtain the n -th individual of the $(g+1)$ -th generation, i.e., $(\nu_i)_n^{g+1}$ and $(u_i)_n^{g+1}$, according to the following rule:

$$\begin{aligned} (\nu_i)_n^{g+1} &= \begin{cases} (\nu_i)_n^g, & \text{if } \text{rand}_i < CR \text{ or } \text{rand} = 1, \\ (\alpha_i)_n^g, & \text{otherwise,} \end{cases} \\ (u_i)_n^{g+1} &= \begin{cases} (u_i)_n^g, & \text{if } \text{rand}_i < CR \text{ or } \text{rand} = 2, \\ (f_i)_n^g, & \text{otherwise,} \end{cases} \end{aligned} \quad (14)$$

where CR is the crossover control parameter and rand_i is a random number uniformly selected between 0 and 1. $\text{rand} \in [1, 2]$ is a randomly selected integer number.

Analysis of boundary condition: To obtain feasible offloading decisions, the boundary absorption method is

utilized to investigate the boundary condition. The boundary absorption of ν_i can be expressed as:

$$\nu_i = \begin{cases} \alpha_i^L, & \text{if } \nu_i < \alpha_i^L, \\ \alpha_i^U, & \text{if } \nu_i > \alpha_i^U, \\ \nu_i, & \text{else.} \end{cases} \quad (15)$$

Note that the detection and absorption rule of u_i can be obtained in the same manner as eq. (15) and is omitted due to space limitations.

Offspring selection: Note that the trial vector is only compared with one individual rather than all individuals. As such, offspring selection can be realized according to the comparison between the trial vector and the current target vector, where the vector with the minimum objective function mentioned in P1.1 is selected as the offspring. One has:

$$\mathbf{p}_i^{g+1} = \begin{cases} (\boldsymbol{\nu}_i, \mathbf{u}_i)^{g+1}, & \text{if } E^{total}((\boldsymbol{\nu}_i, \mathbf{u}_i)^{g+1}) \\ & \leq E^{total}((\boldsymbol{\alpha}_i, \mathbf{f}_i)^g), \\ (\boldsymbol{\alpha}_i, \mathbf{f}_i)^g, & \text{otherwise.} \end{cases} \quad (16)$$

One can select the individual $(\alpha_i^{g+1}, f_i^{g+1})$ of \mathbf{p}_i^{g+1} with the minimum corresponding value of E^{total} as the offspring. Let ε_{DE}^{th} be the acceptable accuracy parameter of the proposed enhanced DE algorithm. The termination conditions are set to $\varepsilon_{DE}^{g+1} = \frac{|E^{total}(\alpha_i^{g+1}, f_i^{g+1}) - E^{total}(\alpha_i^g, f_i^g)|}{E^{total}(\alpha_i^g, f_i^g)} \leq \varepsilon_{DE}^{th}$ or the maximum number of iterations g^{max} is reached. In this way, one can obtain the feasible α_i^* and f_i^* . Detailed information regarding the proposed EDE algorithm is summarized in Algorithm 1.

Algorithm 1 The proposed EDE algorithm

Inputs: $f_i^{max}, p_i^{tr}, U_i, \boldsymbol{\theta}, \mathbf{w}_i, \varepsilon_{DE}^{th}, g^{max}$

Outputs: α_i^*, f_i^*

- 1: set $q = 0$ and $\varepsilon_1^{(0)} = 1$;
 - 2: randomly generate numbers between $[0, 1]$ to form $\boldsymbol{\rho}$;
 - 3: initialize 0-th generation according to Eq. (11);
 - 4: **while** $\varepsilon_{DE}^g > \varepsilon_{DE}^{th}$ or $g < g^{max}$ **do**
 - 5: mutation $(\boldsymbol{\nu}_i, \mathbf{u}_i)^g$ according to Eq. (12);
 - 6: crossover $(\boldsymbol{\nu}_i, \mathbf{u}_i)^g$ according to Eq. (14);
 - 7: detect the boundary conditions of $(\boldsymbol{\nu}_i, \mathbf{u}_i)^{g+1}$ according to Eq. (15);
 - 8: select the individuals entering the next generation population \mathbf{p}_i^{g+1} according to (16);
 - 9: $\varepsilon_{DE}^{g+1} = \frac{|E^{total}(\alpha_i^{g+1}, f_i^{g+1}) - E^{total}(\alpha_i^g, f_i^g)|}{E^{total}(\alpha_i^g, f_i^g)}$;
 - 10: $g \leftarrow g + 1$;
 - 11: **end while**
 - 12: update $\alpha_i^* = \alpha_i^g, f_i^* = f_i^g$
-

B. The Joint Optimization of θ and \mathbf{w}_i

Given any feasible $\alpha^* = \{\alpha_i^*, i \in \mathcal{N}\}$ and $\mathbf{f} = \{f_i^*, i \in \mathcal{N}\}$, $\mathcal{P}1$ can be reduced as:

$$\begin{aligned} \mathcal{P}1.2 : \min_{\theta, \mathbf{w}_i} & \sum_{i=1}^N ((1 - \alpha_i^*) E_i^l(f_i^*) \\ & + \frac{\alpha_i^* D_i}{B_i \log_2(1 + \frac{p_i^{tr} \|\mathbf{w}_i^H(\mathbf{h}_{d,i} + \mathbf{G}\Theta\mathbf{h}_{r,i})\|^2}{\sum_{j \neq i} p_j^{tr} \|\mathbf{w}_i^H(\mathbf{h}_{d,j} + \mathbf{G}\Theta\mathbf{h}_{r,j})\|^2 + \sigma^2 \|\mathbf{w}_i\|^2})}) \\ \text{s.t.} & \quad \mathcal{C}3. \end{aligned} \quad (17)$$

After removing the constant terms, $\mathcal{P}1.2$ can be simplified:

$$\begin{aligned} \tilde{\mathcal{P}}1.2 : \max_{\theta, \mathbf{w}_i} & \frac{p_i^{tr} \|\mathbf{w}_i^H(\mathbf{h}_{d,i} + \mathbf{G}\Theta\mathbf{h}_{r,i})\|^2}{\sum_{j \neq i} p_j^{tr} \|\mathbf{w}_i^H(\mathbf{h}_{d,j} + \mathbf{G}\Theta\mathbf{h}_{r,j})\|^2 + \sigma^2 \|\mathbf{w}_i\|^2} \\ \text{s.t.} & \quad \mathcal{C}3. \end{aligned} \quad (18)$$

One can observe that $\tilde{\mathcal{P}}1.2$ is still difficult to tackle since optimization variables θ and \mathbf{w}_i are closely coupled. To this respect, we divide $\tilde{\mathcal{P}}1.2$ into two subproblems, i.e., $\tilde{\mathcal{P}}1.2.1$ and $\tilde{\mathcal{P}}1.2.2$. By fixing θ , one can obtain the following unconstrained optimization problem $\tilde{\mathcal{P}}1.2.1$:

$$\tilde{\mathcal{P}}1.2.1 : \min_{\mathbf{w}_i} \frac{\sum_{j \neq i} p_j^{tr} \|\mathbf{w}_i^H(\mathbf{h}_{d,j} + \mathbf{G}\Theta\mathbf{h}_{r,j})\|^2 + \sigma^2 \|\mathbf{w}_i\|^2}{p_i^{tr} \|\mathbf{w}_i^H(\mathbf{h}_{d,i} + \mathbf{G}\Theta\mathbf{h}_{r,i})\|^2}. \quad (19)$$

In same manner with [49], the antenna gain in the direction of interest is assumed as unity. Note that MVDR algorithm can adaptively guarantee the output power of the array unchanged in the desired direction and decrease interference and noise power in other directions to promise the SINR performance [50-51]. As such, we utilize MVDR to obtain the optimal beamforming vector. For simplicity purposes, denote $\mathbf{H} = (\sum_{j \neq i} p_j^{tr} (\mathbf{h}_{d,j} + \mathbf{G}\Theta\mathbf{h}_{r,j})(\mathbf{h}_{d,j} + \mathbf{G}\Theta\mathbf{h}_{r,j})^H) + \sigma^2 \mathbf{I}_M$, where \mathbf{I}_M is the identity matrix of $M \times M$ and $\mathbf{h}_i = \sqrt{p_i^{tr}}(\mathbf{h}_{d,i} + \mathbf{G}\Theta\mathbf{h}_{r,i})$. According to **Proposition 1**, the optimal solution \mathbf{w}_i^* to $\tilde{\mathcal{P}}1.2.1$ can be obtained via MVDR and expressed as $\mathbf{w}_i^* = \frac{\mathbf{H}^{-1}\mathbf{h}_i}{\mathbf{h}_i^H \mathbf{H}^{-1} \mathbf{h}_i}$.

Proposition 1: The optimal solution \mathbf{w}_i to $\tilde{\mathcal{P}}1.2.1$ is $\mathbf{w}_i^* = \frac{\mathbf{H}^{-1}\mathbf{h}_i}{\mathbf{h}_i^H \mathbf{H}^{-1} \mathbf{h}_i}$.

Proof. Note that $\tilde{\mathcal{P}}1.2.1$ cannot directly yield a closed-form solution by applying the conventional MVDR. To make $\tilde{\mathcal{P}}1.2.1$ more tractable, introducing $\mathbf{w}_i^H \mathbf{h}_i = 1$, one can obtain that $\|\mathbf{w}_i^H(\mathbf{h}_{d,j} + \mathbf{G}\Theta\mathbf{h}_{r,j})\|^2 = \mathbf{w}_i^H(\mathbf{h}_{d,j} + \mathbf{G}\Theta\mathbf{h}_{r,j})(\mathbf{h}_{d,j} + \mathbf{G}\Theta\mathbf{h}_{r,j})^H \mathbf{w}_i$. Since $\sigma^2 \|\mathbf{w}_i\|^2 = \mathbf{w}_i^H(\sigma^2 \mathbf{I}_M) \mathbf{w}_i$, the numerator of $\tilde{\mathcal{P}}1.2.1$ can be rewritten as:

$$\begin{aligned} & \sum_{j \neq i} p_j^{tr} \|\mathbf{w}_i^H(\mathbf{h}_{d,j} + \mathbf{G}\Theta\mathbf{h}_{r,j})\|^2 + \sigma^2 \|\mathbf{w}_i\|^2 \\ & = \mathbf{w}_i^H \left(\left(\sum_{j \neq i} p_j^{tr} (\mathbf{h}_{d,j} + \mathbf{G}\Theta\mathbf{h}_{r,j})(\mathbf{h}_{d,j} + \mathbf{G}\Theta\mathbf{h}_{r,j})^H \right) \right. \\ & \quad \left. + \sigma^2 \mathbf{I}_M \right) \mathbf{w}_i. \end{aligned} \quad (20)$$

Let $\mathbf{H} = (\sum_{j \neq i} p_j^{tr} (\mathbf{h}_{d,j} + \mathbf{G}\Theta\mathbf{h}_{r,j})(\mathbf{h}_{d,j} + \mathbf{G}\Theta\mathbf{h}_{r,j})^H) + \sigma^2 \mathbf{I}_M$, one has:

$$\mathbf{w}_i^H (\mathbf{h}_{d,j} + \mathbf{G}\Theta\mathbf{h}_{r,j})(\mathbf{h}_{d,j} + \mathbf{G}\Theta\mathbf{h}_{r,j})^H \mathbf{w}_i = \mathbf{w}_i^H \mathbf{H} \mathbf{w}_i. \quad (21)$$

Let $\mathbf{h}_i = \sqrt{p_i^{tr}}(\mathbf{h}_{d,i} + \mathbf{G}\Theta\mathbf{h}_{r,i})$. The denominator of $\tilde{\mathcal{P}}1.2.1$ can be rewritten as:

$$p_i^{tr} \|\mathbf{w}_i^H(\mathbf{h}_{d,i} + \mathbf{G}\Theta\mathbf{h}_{r,i})\|^2 = \mathbf{w}_i^H \mathbf{h}_i \mathbf{h}_i^H \mathbf{w}_i. \quad (22)$$

Due to $\mathbf{w}_i^H \mathbf{h}_i = 1$, one can obtain that $\mathbf{w}_i^H \mathbf{h}_i \mathbf{h}_i^H \mathbf{w}_i = 1$. The optimization problem $\tilde{\mathcal{P}}1.2.1$ can be rewritten as:

$$\begin{aligned} \dot{\mathcal{P}}1.2.1 : \min_{\mathbf{w}_i} & \mathbf{w}_i^H \mathbf{H} \mathbf{w}_i \\ \text{s.t.} & \quad \mathcal{C}4 : \mathbf{w}_i^H \mathbf{h}_i = 1. \end{aligned} \quad (23)$$

By utilizing the Lagrange multiplier method, the Lagrange function $\mathcal{L}(\mathbf{w}_i)$ can be expressed as:

$$\mathcal{L}(\mathbf{w}_i) = \mathbf{w}_i^H \mathbf{H} \mathbf{w}_i + \lambda (\mathbf{w}_i^H \mathbf{h}_i - 1). \quad (24)$$

Assuming that \mathbf{w}_i^* is the optimal solution to $\dot{\mathcal{P}}1.2.1$, the following can be obtained:

$$\left. \frac{\partial \mathcal{L}}{\partial \mathbf{w}_i} \right|_{\mathbf{w}_i = \mathbf{w}_i^*} = 2\mathbf{H} \mathbf{w}_i^* + \lambda \mathbf{h}_i = 0. \quad (25)$$

Thus, one can obtain that $\mathbf{w}_i^* = -\frac{\lambda}{2} \mathbf{H}^{-1} \mathbf{h}_i$. Since $\mathbf{w}_i^H \mathbf{h}_i = \mathbf{h}_i^H \mathbf{w}_i = 1$, one can observe that $\mathbf{h}_i^H \mathbf{w}_i = \mathbf{h}_i^H (-\frac{\lambda}{2} \mathbf{H}^{-1} \mathbf{h}_i) = 1$. Note that $\mathbf{h}_i^H \mathbf{H}^{-1} \mathbf{h}_i$ is a real number with $-\frac{\lambda}{2} = \frac{1}{\mathbf{h}_i^H \mathbf{H}^{-1} \mathbf{h}_i}$. After substituting it into $\mathbf{w}_i^* = -\frac{\lambda}{2} \mathbf{H}^{-1} \mathbf{h}_i$, the following equation results:

$$\mathbf{w}_i^* = \frac{\mathbf{H}^{-1} \mathbf{h}_i}{\mathbf{h}_i^H \mathbf{H}^{-1} \mathbf{h}_i}. \quad (26)$$

The proof is completed. \square

Substituting \mathbf{w}_i^* into problem $\tilde{\mathcal{P}}1.2$, one has

$$\begin{aligned} \tilde{\mathcal{P}}1.2.2 : \max_{\theta} & \frac{p_i^{tr} \|(\mathbf{w}_i^*)^H(\mathbf{h}_{d,i} + \mathbf{G}\Theta\mathbf{h}_{r,i})\|^2}{\sum_{j \neq i} p_j^{tr} \|(\mathbf{w}_i^*)^H(\mathbf{h}_{d,j} + \mathbf{G}\Theta\mathbf{h}_{r,j})\|^2 + \sigma^2 \|\mathbf{w}_i^*\|^2} \\ \text{s.t.} & \quad \mathcal{C}3. \end{aligned} \quad (27)$$

One can observe that $\tilde{\mathcal{P}}1.2.2$ is a non-convex optimization problem and cannot be solved efficiently. As proved in [52], MM algorithm has numerous advantages over than widely used semidefinite relaxation algorithm to handle the formulated problem due to its appealing features, such as fast speed, stability and lower computational complexity. Inspired by the traditional MM algorithm, the enhanced MM algorithm (EMM) is proposed to solve $\tilde{\mathcal{P}}1.2.2$. Define $\mathbf{v} = \mathbf{G} \text{diag}(\mathbf{h}_{r,i}) \in \mathbb{C}^{M \times K}$, $\Phi = [\Phi_1, \Phi_2, \dots, \Phi_K]^T$, $\Phi_k = e^{j\theta_k}$ and $Q = \mathbf{h}_{d,i}^H \mathbf{w}_i^* (\mathbf{w}_i^*)^H \mathbf{h}_{d,i}$, which is a constant. As such, the numerator of $\tilde{\mathcal{P}}1.2.2$ can be rewritten as:

where step (a) exploits $R = \Phi^H \Phi$ and step (b) grasps $\mathbf{X} = p_i^{tr} \mathbf{v}^H \mathbf{w}_i^* (\mathbf{w}_i^*)^H \mathbf{h}_{d,i} \in \mathbb{C}^{K \times 1}$ and $\mathbf{Y} = p_i^{tr} \left[\frac{Q}{R} \mathbf{I}_K + \mathbf{v}^H \mathbf{w}_i^* (\mathbf{w}_i^*)^H \mathbf{v} \right] \in \mathbb{C}^{K \times K}$.

Define $\mathbf{A} = \sum_{j \neq i} p_j^{tr} \mathbf{Y}_j + \frac{\sigma^2}{R} \mathbf{I}_K$ and $\mathbf{B} = \sum_{j \neq i} p_j^{tr} \mathbf{X}_j$, the denominator of objective function mentioned in $\tilde{\mathcal{P}}1.2.2$ can be rewritten as $\sum_{j \neq i} p_j^{tr} \|(\mathbf{w}_i^*)^H(\mathbf{h}_{d,j} + \mathbf{G}\Theta\mathbf{h}_{r,j})\|^2 + \sigma^2 = \Phi^H \mathbf{A} \Phi + 2\text{Re}\{\Phi^H \mathbf{B}\}$. As such, the objective function of

$$p_i^{tr} \|(\mathbf{w}_i^*)^H (\mathbf{h}_{d,i} + \mathbf{G}\Theta \mathbf{h}_{r,i})\|^2 = p_i^{tr} [(\mathbf{h}_{d,i}^H + \Phi^H \mathbf{v}^H) \mathbf{w}_i^*] [(\mathbf{w}_i^*)^H (\mathbf{h}_{d,i} + \mathbf{v}\Phi)] \quad (28)$$

$$= p_i^{tr} [Q + \mathbf{h}_{d,i}^H \mathbf{w}_i^* (\mathbf{w}_i^*)^H \mathbf{v}\Phi + \Phi^H \mathbf{v}^H \mathbf{w}_i^* (\mathbf{w}_i^*)^H \mathbf{h}_{d,i} + \Phi^H \mathbf{v}^H \mathbf{w}_i^* (\mathbf{w}_i^*)^H \mathbf{v}\Phi] \quad (29)$$

$$\stackrel{(a)}{=} p_i^{tr} [\Phi^H (\frac{Q}{R} \mathbf{I}_k + \mathbf{v}^H \mathbf{w}_i^* (\mathbf{w}_i^*)^H \mathbf{v}) \Phi + \mathbf{h}_{d,i}^H \mathbf{w}_i^* (\mathbf{w}_i^*)^H \mathbf{v}\Phi + \Phi^H \mathbf{v}^H \mathbf{w}_i^* (\mathbf{w}_i^*)^H \mathbf{h}_{d,i}] \quad (30)$$

$$\stackrel{(b)}{=} \Phi^H \mathbf{Y}\Phi + 2Re\{\Phi^H \mathbf{X}\}, \quad (31)$$

$\tilde{\mathcal{P}}1.2.2$ can be rewritten as $\frac{\Phi^H \mathbf{Y}\Phi + 2Re\{\Phi^H \mathbf{X}\}}{\Phi^H \mathbf{A}\Phi + 2Re\{\Phi^H \mathbf{B}\}}$, which is defined as the function $f(\Phi)$. In this way, $\mathcal{P}1.2.2$ can be rewritten as:

$$\tilde{\mathcal{P}}1.2.2: \max_{\Phi} f(\Phi) \quad (32)$$

$$s.t. \ C5: \|\Phi_k\| = 1, k = 1, 2, \dots, K.$$

According to **Proposition 2**, one can obtain the lower bound of the objective function $f(\Phi)$ of $\tilde{\mathcal{P}}1.2.2$.

Proposition 2: The lower bound of $f(\Phi)$ can be given as

$$\begin{aligned} f(\Phi) &= C_1 + C_2 + \frac{2Re\{\Phi_0^H (\mathbf{Y} + \frac{2}{R} Re\{\Phi_0 \mathbf{X}\} \mathbf{I}_k) \Phi\}}{\Phi_0^H \mathbf{A}\Phi_0 + 2Re\{\Phi_0^H \mathbf{B}\}} \\ &- \frac{\Phi_0^H \mathbf{Y}\Phi_0 + 2Re\{\Phi_0^H \mathbf{X}\}}{(\Phi_0^H \mathbf{A}\Phi_0 + 2Re\{\Phi_0^H \mathbf{B}\})^2} \times [\Phi^H \lambda_{max}(\mathbf{A}) \Phi \\ &+ 2Re\{\Phi^H (\mathbf{A} - \lambda_{max}(\mathbf{A}) \mathbf{I}_k) \Phi_0\} + 2Re\{\Phi^H \mathbf{B}\}], \end{aligned} \quad (33)$$

where $\lambda_{max}(\mathbf{A})$ is the maximum eigenvalue of \mathbf{A} , Φ_0 is a feasible point and

$$\begin{aligned} C_1 &= \frac{\Phi_0^H \mathbf{Y}\Phi_0 + 2Re\{\Phi_0^H \mathbf{X}\}}{\Phi_0^H \mathbf{A}\Phi_0 + 2Re\{\Phi_0^H \mathbf{B}\}} + \frac{2Re\{\Phi_0^H \mathbf{Y}\Phi_0 + 2Re\{\Phi_0 \mathbf{X}\}\}}{\Phi_0^H \mathbf{A}\Phi_0 + 2Re\{\Phi_0^H \mathbf{B}\}} \\ &+ \frac{\Phi_0^H \mathbf{Y}\Phi_0 + 2Re\{\Phi_0^H \mathbf{X}\}}{(\Phi_0^H \mathbf{A}\Phi_0 + 2Re\{\Phi_0^H \mathbf{B}\})^2} \times (\Phi_0^H \mathbf{A}\Phi_0 + 2Re\{\Phi_0^H \mathbf{B}\}), \\ C_2 &= \frac{\Phi_0^H \mathbf{Y}\Phi_0 + 2Re\{\Phi_0^H \mathbf{X}\}}{(\Phi_0^H \mathbf{A}\Phi_0 + 2Re\{\Phi_0^H \mathbf{B}\})^2} \times (\Phi_0^H (\lambda_{max}(\mathbf{A}) \mathbf{I}_k - \mathbf{A}) \Phi_0). \end{aligned} \quad (34)$$

Proof. Define $\Sigma = \Phi^H \mathbf{A}\Phi + 2Re\{\Phi^H \mathbf{B}\}$ as an intermediate variable. As proved in [53], the function $f(\mathbf{a}, \mathbf{b}) = \mathbf{a}^H \mathbf{b}^{-1} \mathbf{a}$ is jointly convex with (\mathbf{a}, \mathbf{b}) when $\mathbf{b} > \mathbf{0}$. To this respect, $\mathbf{Y} + \frac{2}{R} Re\{\Phi \mathbf{X}\} \mathbf{I}_k$ is positive definite and $\Sigma > 0$. As such, $f(\Phi, \Sigma)$ is jointly convex with (Φ, Σ) . In addition, since the lower bound of a convex function is its first-order Taylor expansion, and thus one has [54]

$$\begin{aligned} f(\Phi, \Sigma) &\geq f(\Phi_0, \Sigma_0) \\ &+ \frac{2Re\{\Phi_0^H (\mathbf{Y} + \frac{2}{R} Re\{\Phi_0 \mathbf{X}\} \mathbf{I}_k) (\Phi - \Phi_0)\}}{\Sigma_0} \\ &- \frac{\Phi_0^H \mathbf{Y}\Phi_0 + 2Re\{\Phi_0^H \mathbf{X}\}}{\Sigma_0^2} (\Sigma - \Sigma_0) \\ &= C_1 + \frac{2Re\{\Phi_0^H (\mathbf{Y} + \frac{2}{R} Re\{\Phi_0 \mathbf{X}\} \mathbf{I}_k) \Phi\}}{\Sigma_0} \\ &- \frac{\Phi_0^H \mathbf{Y}\Phi_0 + 2Re\{\Phi_0^H \mathbf{X}\}}{\Sigma_0^2} \times \Sigma, \end{aligned} \quad (35)$$

where Σ_0 is the corresponding value of Σ under given Φ_0 . By Introducing a $K \times K$ Hermitian matrix $\lambda_{max}(\mathbf{A}) \mathbf{I}_k$ that satisfying $\lambda_{max}(\mathbf{A}) \mathbf{I}_k \geq \mathbf{A}$. According to [55, Lemma 1], one has the following inequality:

$$\begin{aligned} f(\Phi, \Sigma) &\geq C_1 + \frac{2Re\{\Phi_0^H (\mathbf{Y} + \frac{2}{R} Re\{\Phi_0 \mathbf{X}\} \mathbf{I}_k) \Phi\}}{\Sigma_0} \\ &- \frac{\Phi_0^H \mathbf{Y}\Phi_0 + 2Re\{\Phi_0^H \mathbf{X}\}}{\Sigma_0^2} \times [\Phi^H \lambda_{max}(\mathbf{A}) \mathbf{I}_k \Phi \\ &+ \Phi_0^H (\lambda_{max}(\mathbf{A}) \mathbf{I}_k - \mathbf{A}) \Phi_0 \\ &+ 2Re\{\Phi^H (\mathbf{A} - \lambda_{max}(\mathbf{A}) \mathbf{I}_k) \Phi_0\} + 2Re\{\Phi^H \mathbf{B}\}] \\ &= C_1 + C_2 + \frac{2Re\{\Phi_0^H (\mathbf{Y} + \frac{2}{R} Re\{\Phi_0 \mathbf{X}\} \mathbf{I}_k) \Phi\}}{\Phi_0^H \mathbf{A}\Phi_0 + 2Re\{\Phi_0^H \mathbf{B}\}} \\ &- \frac{\Phi_0^H \mathbf{Y}\Phi_0 + 2Re\{\Phi_0^H \mathbf{X}\}}{(\Phi_0^H \mathbf{A}\Phi_0 + 2Re\{\Phi_0^H \mathbf{B}\})^2} \times [\Phi^H \lambda_{max}(\mathbf{A}) \Phi \\ &+ 2Re\{\Phi^H (\mathbf{A} - \lambda_{max}(\mathbf{A}) \mathbf{I}_k) \Phi_0\} + 2Re\{\Phi^H \mathbf{B}\}]. \end{aligned} \quad (36)$$

The proof is completed. \square

Note that the constant term $f(\Phi_0, \Sigma_0)$ affects the value of $f(\Phi, \Sigma)$ under given Φ_0 . Define $\Phi^{(r_{MM})}$ as the value of Φ obtained in iteration r_{MM} ³. To this respect, one can utilize $\Phi^{(r_{MM})}$ to replace Φ_0 by generating a series of feasible vectors. Since $\Phi^H \lambda_{max}(\mathbf{A}) \mathbf{I}_k \Phi = R \lambda_{max}(\mathbf{A})$, C_1 and C_2 are constant terms under certain $\Phi^{(r_{MM})}$, $\tilde{\mathcal{P}}1.2.2$ can be reduced as follows after removing irrelevant constants:

$$\begin{aligned} \tilde{\mathcal{P}}1.2.3: \max_{\Phi} Re\{\Phi^H \mathbf{Z}^{(r_{MM})}\} \\ s.t. \ C5: \|\Phi_k\| = 1, k \in 1, 2, \dots, K, \end{aligned} \quad (37)$$

where

$$\begin{aligned} \mathbf{Z}^{(r_{MM})} &= \frac{(\mathbf{Y}^H + \frac{2}{R} \Phi^{(r_{MM})} \mathbf{X}) \Phi^{(r_{MM})}}{(\Phi^{(r_{MM})})^H \mathbf{A} \Phi^{(r_{MM})} + 2(\Phi^{(r_{MM})})^H \mathbf{B}} \\ &- \frac{(\Phi^{(r_{MM})})^H \mathbf{Y} \Phi^{(r_{MM})} + 2(\Phi^{(r_{MM})})^H \mathbf{X}}{((\Phi^{(r_{MM})})^H \mathbf{A} \Phi^{(r_{MM})} + 2(\Phi^{(r_{MM})})^H \mathbf{B})^2} \\ &\times [(\mathbf{A} - \lambda_{max}(\mathbf{A}) \mathbf{I}_k) \Phi^{(r_{MM})} + \mathbf{B}]. \end{aligned} \quad (38)$$

According to **Proposition 3**, the optimal solution to the optimization problem $\tilde{\mathcal{P}}1.2.3$ can be given as $\Phi^{(r_{MM}+1)} = e^{j \arg\{\mathbf{Z}^{(r_{MM})}\}}$. The termination condition is set to reaching the maximum number of iterations r_{MM}^{max} or $\frac{|E^{total}(\Phi^{(r_{MM}+1)}, \mathbf{w}_i^{(r_{MM}+1)}) - E^{total}(\Phi^{(r_{MM})}, \mathbf{w}_i^{(r_{MM})})|}{E^{total}(\Phi^{(r_{MM})}, \mathbf{w}_i^{(r_{MM})})} \leq \varepsilon_{MM}^{th}$, where ε_{MM}^{th} is the acceptable accuracy parameter. Detailed information of the EMM algorithm is summarized

³For notational simplicity, r_{MM} is the current iteration number as mentioned in Algorithm 2.

in Algorithm 2.

Algorithm 2 The proposed joint IRS phase shift-vector and beamforming vector optimization algorithm.

Inputs: α_i^* , f_i^* , p_i^{tr} , U_i , $\mathbf{h}_{d,i}$, $\mathbf{h}_{r,i}$, ε_{MM}^{th} , r_{MM}^{max}

Outputs: Φ^* , \mathbf{w}_i^*

- 1: set $r_{MM} = 0$ and $\varepsilon_{MM}^{(0)} = 1$;
- 2: initialize $\Phi^{(0)}$ and satisfies $\|\Phi_k\| = 1$;
- 3: **while** $\varepsilon_{MM}^{(r_{MM})} > \varepsilon_{MM}^{th}$ or $r_{MM} < r_{MM}^{max}$ **do**
- 4: substitute α_i^* and f_i^* into $\mathcal{P}1$ to obtain $\mathcal{P}1.2$;
- 5: transform $\mathcal{P}1.2$ into $\tilde{\mathcal{P}}1.2$ by removing constant terms;
- 6: divide $\tilde{\mathcal{P}}1.2$ into $\tilde{\mathcal{P}}1.2.1$ and $\tilde{\mathcal{P}}1.2.2$;
- 7: **The MVDR algorithm:**
- 8: transform $\tilde{\mathcal{P}}1.2.1$ to $\hat{\mathcal{P}}1.2.1$ and utilize MVDR algorithm to solve $\hat{\mathcal{P}}1.2.1$ and obtain \mathbf{w}_i^* ;
- 9: substitute \mathbf{w}_i^* into problem $\tilde{\mathcal{P}}1.2$ to obtain $\tilde{\mathcal{P}}1.2.2$;
- 10: transform problem $\tilde{\mathcal{P}}1.2.2$ into $\hat{\mathcal{P}}1.2.2$;
- 11: **The EMM algorithm:**
- 12: utilize $\Phi^{(r_{MM})}$ to replace Φ_0 , and reformulated $\hat{\mathcal{P}}1.2.2$ into $\tilde{\mathcal{P}}1.2.3$;
- 13: solve $\tilde{\mathcal{P}}1.2.3$ and obtain the optimal $\Phi^{(r_{MM}+1)}$;
- 14: compute $\frac{\varepsilon_{MM}^{(r_{MM}+1)}}{|E^{total}(\Phi^{(r_{MM}+1)}, \mathbf{w}_i^{(r_{MM}+1)}) - E^{total}(\Phi^{(r_{MM})}, \mathbf{w}_i^{(r_{MM})})|} =$
- 15: $\frac{E^{total}(\Phi^{(r_{MM})}, \mathbf{w}_i^{(r_{MM})})}{E^{total}(\Phi^{(r_{MM}+1)}, \mathbf{w}_i^{(r_{MM}+1)})}$;
- 16: **end while**
- 17: update $\Phi^* = \Phi^{(r_{MM})}$, $\mathbf{w}_i^* = \mathbf{w}_i^{(r_{MM})}$

Proposition 3: The optimal solution to the optimization problem $\tilde{\mathcal{P}}1.2.3$ can be given as $\Phi^{(r_{MM}+1)} = e^{j\arg\{\mathbf{Z}^{(r_{MM})}\}}$.

Proof. **Proposition 3** is proved by contradiction. Define $\mathcal{F} = \{\Phi_k | \Phi_k = e^{j\theta_k}, \theta_k \in [0, 2\pi), k \in 1, 2, \dots, K\}$. Let ξ be the angle between any feasible vector Φ and $\mathbf{Z}^{(r_{MM})}$. The project mapping $\mathbf{Z}^{(r_{MM})}$ onto the set \mathcal{F} is the mapping defined by $P_{\mathcal{F}}$. In this way, $\tilde{\mathcal{P}}1.2.3$ can be equivalently transformed into:

$$\begin{aligned} \hat{\mathcal{P}}1.2.3: \quad & \max_{\xi} P_{\mathcal{F}} \mathbf{Z}^{(r_{MM})} \\ \text{s.t.} \quad & \Phi_k \in \mathcal{F}, \quad k = 1, 2, \dots, K. \end{aligned} \quad (39)$$

Assuming that there exist another optimal solution Φ' to $\hat{\mathcal{P}}1.2.3$ with $\Phi' \neq e^{j\arg\{\mathbf{Z}^{(r_{MM})}\}}$ and $\xi \in (0, 2\pi)$. The objective function of $\hat{\mathcal{P}}1.2.3$ can be given by:

$$\begin{aligned} P_{\mathcal{F}} \mathbf{Z}^{(r_{MM})} &= \|\mathbf{Z}^{(r_{MM})}\| \|\Phi'\| \cos \xi = \|\mathbf{Z}^{(r_{MM})}\| \cos \xi \\ &< \|\mathbf{Z}^{(r_{MM})}\| \|\mathbf{Z}^{(r_{MM})}\| \cos 0 \\ &= \|\mathbf{Z}^{(r_{MM})}\| \|\mathbf{Z}^{(r_{MM})}\|. \end{aligned} \quad (40)$$

According to eq. (37), one can observe that there always exists $\Phi = e^{j\arg\{\mathbf{Z}^{(r_{MM})}\}}$ to promise a better solution to $P_{\mathcal{F}} \mathbf{Z}^{(r_{MM})}$ rather than Φ' . As such, the optimal solution to $\tilde{\mathcal{P}}1.2.3$ can be realized if and only if when $\Phi^{(r_{MM}+1)} = e^{j\arg\{\mathbf{Z}^{(r_{MM})}\}}$. The proof is completed. \square

Algorithm 3 The framework of the proposed DMM solution

- 1: initialize α , \mathbf{f} , θ and \mathbf{w}_i ;
- 2: set the iteration number $r = 0$ and the maximum iteration number r^{max} ;
- 3: **repeat**
- 4: **for** $i = 1 : N$ **do**
- 5: fix θ and \mathbf{w}_i to obtain subproblem $\mathcal{P}1.1$;
- 6: utilize Algorithm 1 to solve $\mathcal{P}1.1$ and obtain α_i^* and f_i^* ;
- 7: fix α_i^* and f_i^* to obtain subproblem $\mathcal{P}1.2$;
- 8: utilize Algorithm 2 to solve $\mathcal{P}1.2$ and obtain θ^* and \mathbf{w}_i^* ;
- 9: update θ and \mathbf{w}_i
- 10: **end for**
- 11: $r \leftarrow r + 1$;
- 12: **until** convergence

C. The Complexity Analysis of the Proposed Solution

The overall process to solve $\mathcal{P}1$ is presented in Fig. 3. We first divide $\mathcal{P}1$ into a series of subproblems, e.g., $\mathcal{P}1.1$ and $\mathcal{P}1.2$. To solve the optimization problem $\mathcal{P}1.1$, the EDE algorithm (refer to Algorithm 1) is proposed to optimize integer variable α_i and continuous variable f_i . After obtaining the feasible solutions α_i^* and f_i^* according to Algorithm 1, IRS phase shift-vector θ and beamforming vector \mathbf{w}_i and can be jointly optimized by using Algorithm 2. The overall framework of the proposed heuristic algorithm is summarized in Algorithm 3. In particular, the convergence of the Algorithm 3 is set to $\frac{|[E^{total}(\alpha^*, \mathbf{f}^*, \theta^*, \mathbf{w}_i^*)]^{r+1} - [E^{total}(\alpha^*, \mathbf{f}^*, \theta^*, \mathbf{w}_i^*)]^r|}{[E^{total}(\alpha^*, \mathbf{f}^*, \theta^*, \mathbf{w}_i^*)]^r} \leq \varepsilon$ or the maximum iteration number r^{max} is reached. In this way, one can obtain the suboptimal solution to the challenging formulated problem $\mathcal{P}1$ in an efficient manner. The complexity analysis of Algorithm 3 is summarized in Proposition 4. Note that the proposed DMM runs at the MEC server where the computation resources are sufficient and thus the computation overhead can be negligible [56]. Moreover, the communication overhead can be ignored since each UAV-TBS and TBS-MEC server link is supported by optical fiber and cable, respectively. In addition, TBS can send the optimization parameters, such as offloading decisions and computation capability information to USVs even when the transmission between TBS and USVs is affected by external factors, by temporarily increasing the transmission power.

Proposition 4: The complexity of the proposed DMM solution can be roughly given as $\mathcal{O}(I_r N (I_{EDE} N^2 + I_{MM} (M^3 + K^3)))$, where I_r , I_{EDE} , and I_{MM} denote the number of iterations required for steps 3-12 in Algorithm 3, steps 4-11 in Algorithm 1 and steps 3-14 in Algorithm 2 until convergence, respectively.

Proof. The complexity of Algorithm 1 to solve $\mathcal{P}1.1$ is $\mathcal{O}(I_{EDE} N^2)$. The complexity to obtain the matrix inverse of \mathbf{H} and the maximum eigenvalue of \mathbf{A} is $\mathcal{O}(M^3)$ and $\mathcal{O}(K^3)$, respectively. Therefore, the complexity of Algorithm 2 to solve $\mathcal{P}1.2$ is $\mathcal{O}(I_{MM} (M^3 + K^3))$. As a result, the complexity of Algorithm 3 can be roughly given as $\mathcal{O}(I_r N (I_{EDE} N^2 + I_{MM} (M^3 + K^3)))$. \square

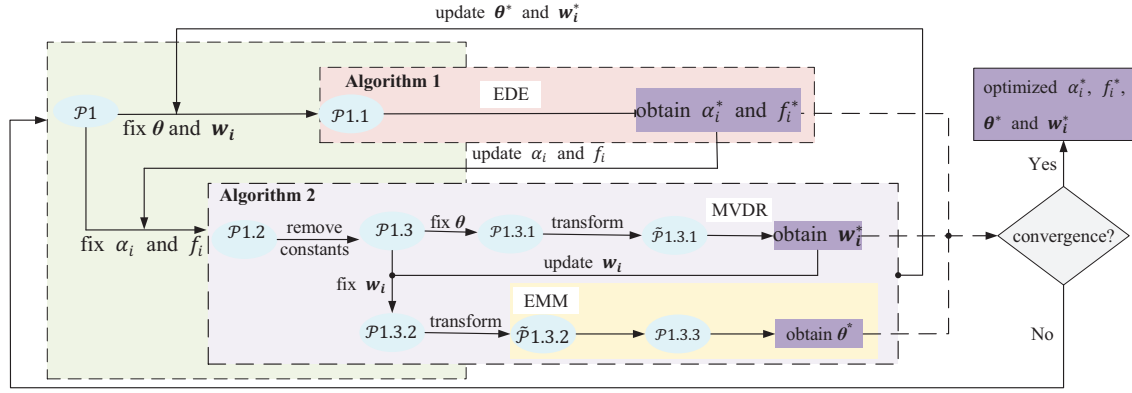
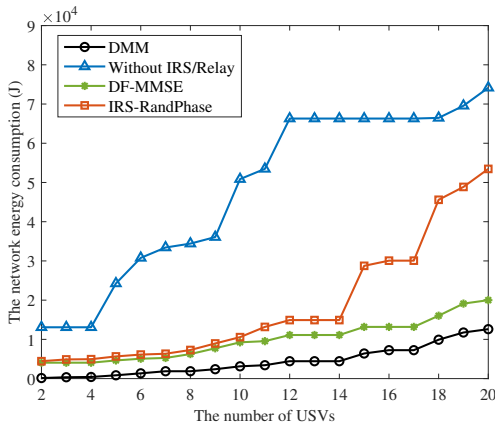

 Fig. 3: The overall process to solve $\mathcal{P}1$.


Fig. 4: The network energy consumption versus the different number of USVs.

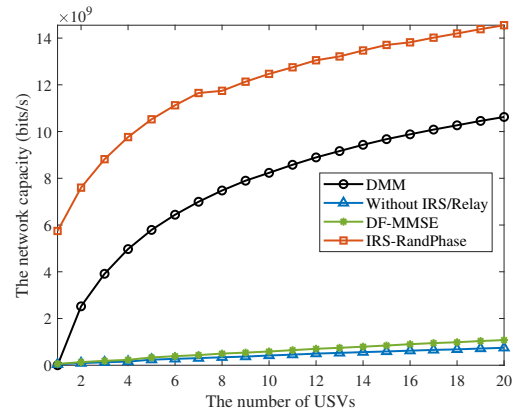


Fig. 5: The network capacity versus the different number of USVs.

V. PERFORMANCE EVALUATION

The simulation setup of the proposed IRS-assisted hybrid UAV-terrestrial MEC network with USVs is described as follows. USVs are randomly distributed in a circular area with a radius of 75 meters (m) and UAV flies at a fixed altitude of $H = 10$ m. Each USV generates 50 tasks. The maximum computation capability of each USV and MEC server are set as $f_i^{max} = 5 \times 10^5$ and $f_m = 1 \times 10^7$ CPU cycles/s, respectively. k_i and ζ_i are set as 10^{-11} and 2, respectively. In this paper, we assume that channels are follow small-scale fading, which can be given by

$$G_r = G_{r_0} - 10\eta \log_{10}\left(\frac{d}{d_0}\right), \quad (41)$$

where $G_{r_0} = 30$ dB is the path loss (PL) at the reference distance $d_0 = 1$ m. USV-UAV link is assumed as a controllable LoS channel when utilizing IRS technique. UAV-TBS link and USV-TBS link are assumed as LoS and non-LoS, respectively [57]. η indicates the PL coefficients, where USV-TBS link, IRS-TBS link and USV-UAV link are set to 3.5, 2.2, 2.2, respectively. The noise power σ^2 is -70 dBm and the channel bandwidth is 1 MHz. The convergence accuracy parameters ε_{DE}^{th} , ε_{MM}^{th} and ε are set as 10^{-3} . In the same manner with [58], wireless communication channels are

assumed to be perfectly estimated. Let the total time cost to execute U_i via IRS-assisted offloading be T_i^{IO} . Note that when $T_i \leq \{T_i^l, T_i^{IO}\}$, $i \in \mathcal{N}$, U_i is regarded as failed and cannot be allocated any computation resources or bandwidth. The selected up-to-date advanced algorithms, e.g., the DF-MMSE algorithm, the IRS-RandPhase algorithm and the Without IRS algorithm, are selected as benchmarks. Most significant information regarding these algorithms is summarized as follows.

DF-MMSE algorithm: The energy efficient method, called the relay-assisted based algorithm (refer to DF-MMSE in the following), is selected. In particular, this approach utilizes a DF relay to assist task offloading and applies the minimum mean-square error (MMSE) method to design TBS beamforming vector as mentioned in [59].

IRS-RandPhase algorithm: The random phase algorithm (refer to RandPhase in the following) aims to maximize the number of offloaded tasks by randomly generates IRS phase shift-vector and TBS beamforming vector.

Without IRS/Relay algorithm: The without IRS algorithm (refer to Without IRS/Relay in the following) do not utilize IRS and thus set $\mathbf{G}\Theta\mathbf{h}_{r,i} = 0$. The optimization of USVs offloading decision and computation capability is in the same manner with Algorithm 1 and the TBS beamforming vector design follows MVDR algorithm as mentioned in Algorithm

2.

For simplification, the network energy consumption is defined as the total energy consumption of USVs. The network energy consumption versus the different number of USVs is shown in Fig. 4 when $K = 75$ and $p_i^{tr} = 2$ W. One can observe that with the increase of USVs, the network energy consumption correspondingly increases. In particular, DMM realizes the lowest network energy consumption at nearly 1.35×10^4 J (Joule) and 2×10^3 J when $N = 20$ and $N = 5$, respectively, where the corresponding value of the DF-MMSE algorithm is about 2.1×10^4 J and 3.8×10^3 J. Followed by the IRS-RandPhase algorithm with the corresponding values at about 5.5×10^4 J and 4×10^3 J, respectively. The Without IRS/Relay algorithm realizes the worst performance, with the network energy consumption around 8.5×10^4 J when $N = 20$. This is because DMM solution can jointly optimize the beamforming vector \mathbf{w}_i and IRS phase shift-vector $\boldsymbol{\theta}$. In this way, the channel capacity can be significantly enhanced while the offloading time cost of USVs can be reduced. As a result, the proposed algorithm outperforms the IRS-RandPhase algorithm regarding network energy consumption. Moreover, one can observe that network energy consumption can be significantly decreased by utilizing IRS-assisted transmission compared with the DF-MMSE and Without IRS/Relay algorithm.

The relationship between the network capacity versus the number of USVs is demonstrated in Fig. 5 when $K = 75$ and $p_i^{tr} = 2$ W. As can be seen from Fig. 5, the proposed algorithm achieves a higher network capacity than the Without IRS algorithm under the same number of USVs. In particular, the network capacity of the proposed algorithm is approximately 10.6×10^9 bits/s and 5.9×10^9 bits/s when $N = 20$ and $N = 5$, respectively. The Without IRS algorithm realizes the network capacity at around 1.7×10^9 bits/s and 2.4×10^8 bits/s when $N = 20$ and $N = 5$, respectively. Note that although DMM solution can promise lower network energy consumption compared with the IRS-RandPhase algorithm, this may result in sacrificing the SINR performance and decreasing the network capacity.

Fig. 6 and Fig. 7 plot the number of IRS-assisted offloading tasks versus the number of USVs and IRS elements, respectively. As shown in Fig. 6, as the number of USVs increases, the number of USVs that select the IRS-assisted offloading method increases correspondingly. In particular, the number of IRS-assisted offloading tasks of the DMM solution is about 510 when $N = 10$ while this value is around 105 for the IRS-RandPhase algorithm. This is because the proposed algorithm can optimize IRS phase shift-vector; USVs are highly likely to select IRS-assisted offloading method with the lower energy consumption rather than local execution. One can observe from Fig. 7 that a larger number of IRS elements promises a higher number of IRS-assisted offloading tasks. In particular, when $K = 50$, the number of IRS-assisted offloading tasks for the proposed algorithm is nearly 225 while this value is around 128 for the IRS-RandPhase algorithm. This is because the DMM solution realizes the higher spatial degree-of-freedom compared with the IRS-RandPhase algorithm, which promises a higher number of tasks that can be successfully executed via IRS-assisted offloading method.

To balance the number of USVs and IRS elements, we select $N = 5$ for further discussion. Fig. 8 shows the network energy consumption versus the number of IRS elements under the typical computation capability of MEC server when employing the proposed algorithm and the IRS-RandPhase algorithm. One can observe that a higher number of IRS elements results in lower network energy consumption for both algorithms. Moreover, the DMM solution outperforms the IRS-RandPhase algorithm when utilizing the same number of IRS elements. In particular, the DMM solution realizes the network energy consumption around 2×10^3 J when $K = 75$ and $f_m = 10^7$ CPU cycles/s while this value is nearly 1.6×10^4 J when $f_m = 10^6$ CPU cycles/s. This may involve the fact that MEC execution time can be significantly decreased with higher computation capability. As such, the proposed algorithm encourages a higher number of USVs to offload tasks to MEC server for execution, which in turn decreases the network energy consumption.

Fig. 9 and Fig. 10 show the network energy consumption of the proposed algorithm under different numbers of USVs and IRS elements, respectively. One can observe that the network energy consumption increases with USVs transmission power rise. According to Fig. 9, the network energy consumption is almost 3.2×10^4 J when $N = 20$ and $p_i^{tr} = 5$ W while this value is nearly 5.3×10^3 J when $p_i^{tr} = 0.5$ W. According to Fig. 10, when $K = 50$ and $p_i^{tr} = 5$ W, the network energy consumption is approximately 2.7×10^4 J, while this value is about 2.1×10^3 J when $K = 100$. As such, in the case of higher transmission power, one can reduce the network energy consumption by increasing the number of IRS elements, especially when the number of IRS elements is less than 50. Moreover, one should aware that increasing the transmission power of USVs promises better transmission quality while suffering additional energy consumption.

The proposed DMM solution has numerous practical advantages in comparison with existing state of the art algorithms. In this paper, we assume that each task is indivisible and can either be executed by USV itself or offloaded to MEC server via IRS-assisted offloading method according to the dynamic communication environment. Moreover, the proposed algorithm assumes that each USV follows the same range of computation capability, i.e., $[f_i^{min}, f_i^{max}]$. In this regard, the computation capabilities of USVs need to be dynamically determined rather than determined as fixed values as studied in [60-61]. In addition, unlike [60], the proposed algorithm can optimize each USV's computation capability to avoid energy waste. Furthermore, the joint optimization of beamforming vectors of each USV i and IRS phase shift-vector is taken into consideration. In this way, IRS is capable of adjusting its phase shift dedicatedly for its associated USV to enhance the channel condition. The performance of the proposed algorithm regarding the different number of USVs and IRS elements are respectively presented. The fact that the simulation results show that the proposed DMM algorithm achieves better performance in comparison with several state-of-the-art algorithms indicates that DMM gets closer to the optimum solution than the other energy efficient algorithms.

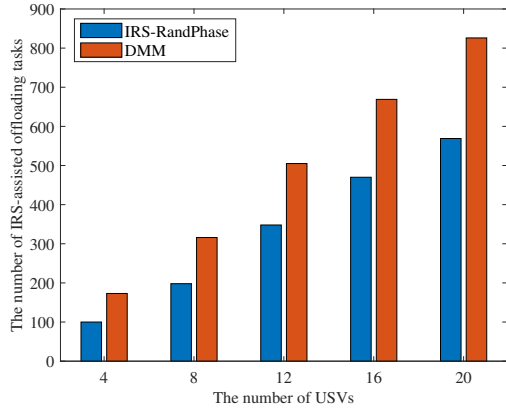


Fig. 6: The number of IRS-assisted offloading tasks versus the different number of USVs.

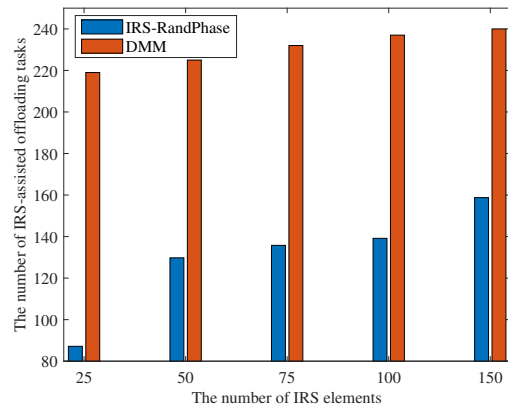


Fig. 7: The number of IRS-assisted offloading tasks versus the different number of IRS elements.

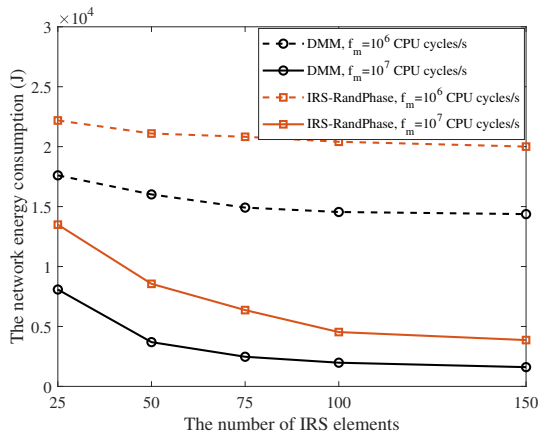


Fig. 8: The network energy consumption versus the different number of IRS elements under different typical computation capability of MEC server.

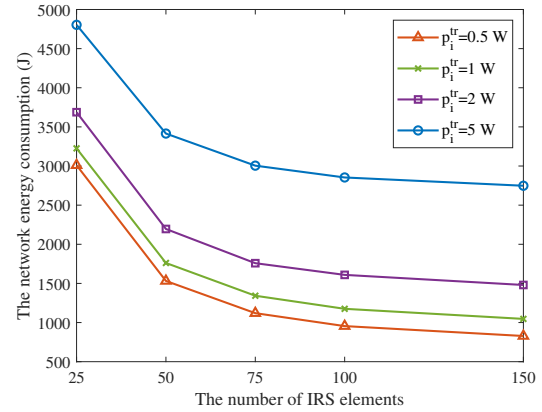


Fig. 10: The network energy consumption versus the different number of IRS elements under different typical USV transmission power.

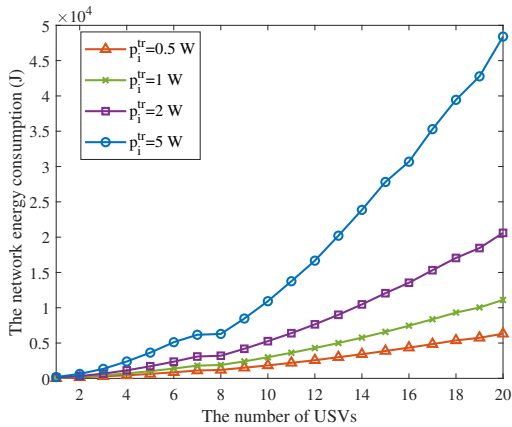


Fig. 9: The network energy consumption versus the different number of USVs under different typical USV transmission power.

VI. CONCLUSIONS

This paper proposed an IRS-assisted hybrid UAV-terrestrial MEC network architecture with USVs to reduce energy consumption and increase network capacity. The energy consumption minimization problem of USVs is formulated by jointly considering USVs' offloading decision, computation capability, IRS phase shift-vector and beamforming vector design, which is a non-linear non-convex optimization problem and challenging to solve. To solve the formulated problem, the original optimization problem was divided into two sub-problems and a heuristic solution named DMM was proposed. Part of DMM, the enhanced DE algorithm was introduced to solve USVs offloading decisions and computation capability subproblem, and the MVDR and the enhanced MM algorithms were used to solve the joint IRS phase shift-vector and beamforming vector design subproblem. Simulation results have demonstrated the efficiency of the proposed algorithm in terms of multiple aspects. In particular, the proposed algorithm achieves higher energy efficiency than existing solutions: DF-MMSE, IRS-RandPhase and an Without IRS/Relay approach.

Additionally, DMM testing results have shown that the IRS-assisted offloading method can obtain a higher network capacity than existing algorithms. Furthermore, the proposed algorithm completes a higher number of IRS-assisted offloading tasks than the IRS-RandPhase algorithm.

Future work will consider the evaluation of the solution performance also from a quality of experience (QoE) perspective in a multimedia data transmission context. QoE can be estimated using several components, which include the bitrate of the transmitted video, stall time caused by network delay, degradation of video quality due to variation across consecutive segments and waiting time for the video to start the playout when the transmission begins [62-63]. In addition, although intuitive heuristics have been proposed for IRS deployments [64-65], performing a comprehensive mathematical formulation for multiple IRS placements and optimization based on long-term statistical-computed and/or estimated CSI values is still an open research problem. Moreover, the optimization of IRS reflecting elements number still needs further research since when multiple IRSs are deployed to serve a list of USVs, the optimal IRS association strategy is generally still unknown according to the current literature [66-68]. This may also influence the flight time and energy consumption of UAVs since the motors consume the higher propulsion and hovering power to keep the total weight in the air, especially for non-tethered UAVs that rely on on-board batteries [69].

REFERENCES

- [1] Nokia Networks, "White Paper-5G Use Cases and Requirements Future Works," Tech. Rep, 2014.
- [2] A. Dogra, R. K. Jha and S. Jain, "A Survey on Beyond 5G Network With the Advent of 6G: Architecture and Emerging Technologies," *IEEE Access*, vol. 9, pp. 67512-67547, Oct. 2021.
- [3] L. Zhang, Y. Liang and D. Niyato, "6G Visions: Mobile Ultra-broadband, Super Internet-of-Things, and Artificial Intelligence," *China Communications*, vol. 16, no. 8, pp. 1-14, Aug. 2019.
- [4] Y. Ma, M. Hu and X. Yan, "Multi-Objective Path Planning for Unmanned Surface Vehicle with Currents Effects," *ISA Transactions*, vol. 75, pp. 137-156, Apr. 2018.
- [5] G. Shao, Y. Ma, R. Malekian, X. Yan and Z. Li, "A Novel Cooperative Platform Design for Coupled USV-UAV Systems," *IEEE Transactions on Industrial Informatics*, vol. 15, no. 9, pp. 4913-4922, Sept. 2019.
- [6] M. Renzo *et al.*, "Smart Radio Environments Empowered by Reconfigurable AI Meta-surfaces: An Idea Whose Time Has Come," *EURASIP J. Wireless Commun. Netw.*, vol. 2019, pp. 1-20, May. 2019.
- [7] C. Liaskos, S. Nie, A. Tsioliaridou, A. Pitsillides, S. Ioannidis and I. Akyildiz, "Realizing Wireless Communication Through Software-Defined HyperSurface Environments," in *IEEE International Symposium on A World of Wireless, Mobile and Multimedia Networks*, Chania, Greece, pp. 14-15, June. 2018.
- [8] S. Ma, W. Guo, R. Song, Y. Liu, "Unsupervised Learning based Coordinated Multi-task Allocation for Unmanned Surface Vehicles," *Neurocomputing*, pp. 227-245, Jan. 2021.
- [9] Y. Liao, X. Chen, S. Xia, Q. Ai and Q. Liu, "Energy Minimization for UAV Swarm-Enabled Wireless Inland Ship MEC Network With Time Windows," *IEEE Transactions on Green Communications and Networking*, vol. 7, no. 2, pp. 594-608, Jun. 2023.
- [10] N. Hassan, K. A. Yau and C. Wu, "Edge Computing in 5G: A Review," *IEEE Access*, vol. 7, pp. 127276-127289, Aug. 2019.
- [11] W. Shi, J. Cao, Q. Zhang, Y. Li and L. Xu, "Edge Computing: Vision and Challenges," *IEEE Internet of Things Journal*, vol. 3, no. 5, pp. 637-646, Oct. 2016.
- [12] Y. Mao, C. You, J. Zhang, K. Huang and K. B. Letaief, "A Survey on Mobile Edge Computing: The Communication Perspective," *IEEE Communications Surveys & Tutorials*, vol. 19, no. 4, pp. 2322-2358, Aug. 2017.
- [13] S. Kosta, A. Aucinas, H. Pan, R. Mortier and X. Zhang, "ThinkAir: Dynamic Resource Allocation and Parallel Execution in the Cloud for Mobile Code Offloading," *IEEE INFOCOM*, Orlando, FL, pp. 945-953, Mar. 2012.
- [14] M. Li, X. Zhou, T. Qiu, Q. Zhao and K. Li, "Multi-relay Assisted Computation Offloading for Multi-access Edge Computing Systems with Energy Harvesting," *IEEE Transactions on Vehicular Technology*, vol. 70, no. 10, pp. 10941-10956, Oct. 2021.
- [15] H. Yang *et al.*, "A Programmable Metasurface with Dynamic Polarization Scattering and Focusing Control," *Scientific Reports*, vol. 6, pp. 35692, Oct. 2016.
- [16] J. Ren, G. Yu, Y. Cai and Y. He, "Latency Optimization for Resource Allocation in Mobile-Edge Computation Offloading," *IEEE Transactions on Wireless Communications*, vol. 17, no. 8, pp. 5506-5519, Aug. 2018.
- [17] J. Qiu, R. Wang, A. Chakrabarti, R. Guérin and C. Lu, "Adaptive Edge Offloading for Image Classification Under Rate Limit," *IEEE Transactions on Computer-Aided Design of Integrated Circuits and Systems*, vol. 41, no. 11, pp. 3886-3897, Nov. 2022.
- [18] K. Wang, K. Yang and C. S. Magurawalage, "Joint Energy Minimization and Resource Allocation in C-RAN with Mobile Cloud," *IEEE Transactions on Cloud Computing*, vol. 6, no. 3, pp. 760-770, July. 2018.
- [19] M. Abrar, U. Ajmal, Z. M. Almohaimed, X. Gui, R. Akram and R. Masroor, "Energy Efficient UAV-Enabled Mobile Edge Computing for IoT Devices: A Review," *IEEE Access*, vol. 9, pp. 127779-127798, Sept. 2021.
- [20] C. Zhan, H. Hu, X. Sui, Z. Liu and D. Niyato, "Completion Time and Energy Optimization in the UAV-Enabled Mobile-Edge Computing System," *IEEE Internet of Things Journal*, vol. 7, no. 8, pp. 7808-7822, Aug. 2020.
- [21] K. Sundaresan, E. Chai, A. Chakraborty and S. Rangarajan, "SkyLiTE: End-to-End Design of Low-Altitude UAV Networks for Providing LTE Connectivity," *arXiv:1802.06042*, Feb. 2018.
- [22] S. Joo, H. Kang and J. Kang, "CoSMoS: Cooperative Sky-Ground Mobile Edge Computing System," *IEEE Transactions on Vehicular Technology*, vol. 70, no. 8, pp. 8373-8377, Aug. 2021.
- [23] Z. Xie, X. Song, J. Cao and W. Qiu, "Providing Aerial MEC Service in Areas Without Infrastructure: A Tethered-UAV-Based Energy-Efficient Task Scheduling Framework," *IEEE Internet of Things Journal*, vol. 9, no. 24, pp. 25223-25236, Dec. 2022.
- [24] C. Huang, A. Zappone, G. C. Alexandropoulos, M. Debbah and C. Yuen, "Reconfigurable Intelligent Surfaces for Energy Efficiency in Wireless Communication," *IEEE Transactions on Wireless Communications*, vol. 18, no. 8, pp. 4157-4170, Aug. 2019.
- [25] W. Zhang, J. Xu, W. Xu, D. W. K. Ng and H. Sun, "Cascaded Channel Estimation for IRS-Assisted mmWave Multi-Antenna With Quantized Beamforming," *IEEE Communications Letters*, vol. 25, no. 2, pp. 593-597, Feb. 2021.
- [26] E. Björnson, Ö. Özdogan and E. G. Larsson, "Intelligent Reflecting Surface Versus Decode-and-Forward: How Large Surfaces are Needed to Beat Relaying?," *IEEE Wireless Communications Letters*, vol. 9, no. 2, pp. 244-248, Feb. 2020.
- [27] P. Q. Huang, Y. Wang, K. Wang and Q. Zhang, "Combining Lyapunov Optimization With Evolutionary Transfer Optimization for Long-Term Energy Minimization in IRS-Aided Communications," *IEEE Transactions on Cybernetics*, vol. 53, no. 4, pp. 2647-2657, April. 2023.
- [28] Y. Cao and T. Lv, "Intelligent Reflecting Surface Enhanced Resilient Design for MEC Offloading Over Millimeter Wave Links," *arXiv:1912.06361*, Dec. 2019.
- [29] Q. Wu *et al.*, "A Comprehensive Overview on 5G-and-Beyond Networks with UAVs: From Communications to Sensing and Intelligence," *IEEE Journal on Selected Areas in Communications*, vol. 39, no. 10, pp. 2912-2945, Oct. 2021.
- [30] S. Jiao, F. Fang, X. Zhou and H. Zhang, "Joint Beamforming and Phase Shift Design in Downlink UAV Networks with IRS-Assisted NOMA," *Journal of Communications and Information Networks*, vol. 5, no. 2, pp. 138-149, June. 2020.
- [31] M. Asim, M. ELAffendi and A. A. A. El-Latif, "Multi-IRS and Multi-UAV-Assisted MEC System for 5G/6G Networks: Efficient Joint Trajectory Optimization and Passive Beamforming Framework," *IEEE Transactions on Intelligent Transportation Systems*, vol. 24, no. 4, pp. 4553-4564, Apr. 2023.
- [32] G. Chen and Q. Wu, "IRS Aided MEC Systems with Binary Offloading: A Unified Framework for Dynamic IRS Beamforming," *IEEE Journal on Selected Areas in Communications*, vol. 41, no. 2, pp. 349-365, Feb. 2022.
- [33] C. Sun, W. Ni, Z. Bu and X. Wang, "Energy Minimization for Intelligent Reflecting Surface-Assisted Mobile Edge Computing," *IEEE Transac-*

- tions on Wireless Communications, vol. 21, no. 8, pp. 6329-6344, Aug. 2022.
- [34] S. Gong *et al.*, "Toward Smart Wireless Communications via Intelligent Reflecting Surfaces: A Contemporary Survey," IEEE Communications Surveys & Tutorials, vol. 22, no. 4, pp. 2283-2314, June. 2020.
- [35] R. Schroeder, J. He and M. Juntti, "Passive RIS vs. Hybrid RIS: A Comparative Study on Channel Estimation," in IEEE Vehicular Technology Conference (VTC2021-Spring), Helsinki, Finland, pp. 1-7, April. 2021.
- [36] J. Xu, L. Yuan, N. Yang, N. Yang and Y. Guo, "Performance Analysis of STAR-IRS Aided NOMA Short-Packet Communications with Statistical CSI," IEEE Transactions on Vehicular Technology, Early Access, doi: 10.1109/TVT.2023.3266830.
- [37] Y. Cao, S. Xu, J. Liu and N. Kato, "Toward Smart and Secure V2X Communication in 5G and Beyond: A UAV-Enabled Aerial Intelligent Reflecting Surface Solution," IEEE Vehicular Technology Magazine, vol. 17, no. 1, pp. 66-73, March. 2022.
- [38] K. Li, K. Zhao, M. F. Khan, P. H. Ho and L. Peng, "UAV-mounted Intelligent Reflecting Surface (IRS) MISO Communications," in International Conference on Networking and Network Applications, Urumqi, China, pp. 62-66, Dec. 2022.
- [39] F. Yang, J. Wang, H. Zhang, M. Lin and J. Cheng, "Multi-IRS-Assisted mmWave MIMO Communication Using Twin-Timescale Channel State Information," IEEE Transactions on Communications, vol. 70, no. 9, pp. 6370-6384, Sept. 2022.
- [40] Q. Tao, S. Zhang, C. Zhong, W. Xu, H. Lin and Z. Zhang, "Weighted Sum-Rate of Intelligent Reflecting Surface Aided Multiuser Downlink Transmission with Statistical CSI," IEEE Transactions on Wireless Communications, vol. 21, no. 7, pp. 4925-4937, July. 2022.
- [41] H. Guo, Y. C. Liang, J. Chen and E. G. Larsson, "Weighted Sum-Rate Maximization for Intelligent Reflecting Surface Enhanced Wireless Networks," IEEE Global Communications Conference, Waikoloa, HI, pp. 1-6, Dec. 2019.
- [42] M. Asim, M. ELAffendi and A. A. A. El-Latif, "Multi-IRS and Multi-UAV-Assisted MEC System for 5G/6G Networks: Efficient Joint Trajectory Optimization and Passive Beamforming Framework," IEEE Transactions on Intelligent Transportation Systems, vol. 24, no. 4, pp. 4553-4564, Apr. 2023.
- [43] Y. Liu, Z. Su and Y. Wang, "Energy-Efficient and Physical-Layer Secure Computation Offloading in Blockchain-Empowered Internet of Things," IEEE Internet of Things Journal, vol. 10, no. 8, pp. 6598-6610, Apr. 2023.
- [44] W. Liu, B. Li, W. Xie, Y. Dai and Z. Fei, "Energy Efficient Computation Offloading in Aerial Edge Networks with Multi-Agent Cooperation," IEEE Transactions on Wireless Communications, Early Access, doi: 10.1109/TWC.2023.3235997.
- [45] R. Storn and K. Price, "Differential Evolution-A Simple and Efficient Heuristic for Global Optimization Over Continuous Spaces," Journal of Global Optimization, vol. 11, no. 4, pp. 341-359, Jan. 1997.
- [46] X. Zhang, Y. Gong, Y. Lin, J. Zhang, S. Kwong and J. Zhang, "Dynamic Cooperative Coevolution for Large Scale Optimization," IEEE Transactions on Evolutionary Computation, vol. 23, no. 6, pp. 935-948, Dec. 2019.
- [47] S. Das, S. S. Mullick, and P. N. Suganthan, "Recent Advances in Differential Evolution-An Updated Survey," Swarm and Evolution Computation, vol. 27, pp. 1-30, Feb. 2016.
- [48] B. Wang, H. Li, J. Li and Y. Wang, "Composite Differential Evolution for Constrained Evolutionary Optimization," IEEE Transactions on Systems, Man, and Cybernetics: Systems, vol. 49, no. 7, pp. 1482-1495, July. 2019.
- [49] F. Rashid-Farrokh, L. Tassiulas and K. J. R. Liu, "Joint Optimal Power Control and Beamforming in Wireless Networks Using Antenna Arrays," IEEE Transactions on Communications, vol. 46, no. 10, pp. 1313-1324, Oct. 1998.
- [50] N. Venkatesh, N. Tandon and A. Jagannatham, "MVDR-Based Multicell Cooperative Beamforming Techniques for Unicast/Multicast MIMO Networks With Perfect/Imperfect CSI," IEEE Transactions on Vehicular Technology, vol. 64, no. 11, pp. 5160-5176, Nov. 2015.
- [51] M. Souden, J. Benesty and S. Affes, "A Study of the LCMV and MVDR Noise Reduction Filters," IEEE Transactions on Signal Processing, vol. 58, no. 9, pp. 4925-4935, Sept. 2010.
- [52] X. Yu, D. Xu and R. Schober, "Enabling Secure Wireless Communications via Intelligent Reflecting Surfaces," IEEE Global Communications Conference, Waikoloa, HI, pp. 1-6, Dec. 2019.
- [53] S. Boyd and L. Vandenberghe, "Convex Optimization," Cambridge, U.K.: Cambridge Univ. Press, 2004.
- [54] A. Hjoungnes, "Complex-Valued Matrix Derivatives: With Applications in Signal Processing and Communications," Cambridge, U.K.: Cambridge Univ. Press, Jan. 2011.
- [55] J. Song, P. Babu and D. P. Palomar, "Optimization Methods for Designing Sequences With Low Autocorrelation Sidelobes," IEEE Transactions on Signal Processing, vol. 63, no. 15, pp. 3998-4009, Aug. 2015.
- [56] D. Tyrovolas, P. V. Mekikis, S. A. Tegos, P. D. Diamantoulakis, C. K. Liaskos and G. K. Karagiannidis, "Energy-Aware Design of UAV-Mounted RIS Networks for IoT Data Collection," IEEE Transactions on Communications, vol. 71, no. 2, pp. 1168-1178, Feb. 2023.
- [57] D. Ma, M. Ding and M. Hassan, "Enhancing Cellular Communications for UAVs via Intelligent Reflective Surface," in IEEE Wireless Communications and Networking Conference, Seoul, Korea, pp. 1-6, May. 2020.
- [58] Q. Wu and R. Zhang, "Intelligent Reflecting Surface Enhanced Wireless Network via Joint Active and Passive Beamforming," IEEE Transactions on Wireless Communications, vol. 18, no. 11, pp. 5394-5409, Nov. 2019.
- [59] F. Benkhalifa, A. S. Salem and M. S. Alouini, "Sum-Rate Enhancement in Multiuser MIMO Decode-and-Forward Relay Broadcasting Channel With Energy Harvesting Relays," IEEE Journal on Selected Areas in Communications, vol. 34, no. 12, pp. 3675-3684, Dec. 2016.
- [60] Q. Ai, X. Qiao, Y. Liao and Q. Yu, "Joint Optimization of USVs Communication and Computation Resource in IRS-Aided Wireless Inland Ship MEC Networks," IEEE Transactions on Green Communications and Networking, vol. 6, no. 2, pp. 1023-1036, June. 2022.
- [61] Z. Sun and Y. Jing, "On the Performance of Multi-Antenna IRS-Assisted NOMA Networks with Continuous and Discrete IRS Phase Shifting," IEEE Transactions on Wireless Communications, vol. 21, no. 5, pp. 3012-3023, May. 2022.
- [62] X. Yin *et al.*, "A Control-theoretic Approach for Dynamic Adaptive Video Streaming over HTTP," in Proceedings of the ACM Conference on Special Interest Group on Data Communication, London, UK, pp. 325-338, Aug. 2015.
- [63] K. Piamrat, C. Viho, J. M. Bonnin and A. Ksentini, "Quality of Experience Measurements for Video Streaming over Wireless Networks," International Conference on Information Technology: New Generations, pp. 1184-1189, Las Vegas, NV, Apr. 2009.
- [64] C. Liaskos, S. Nie, A. Tsioliaridou, A. Pitsillides, S. Ioannidis and I. Akyildiz, "A New Wireless Communication Paradigm through Software-Controlled Metasurfaces," IEEE Communications Magazine, vol. 56, no. 9, pp. 162-169, Sept. 2018.
- [65] S. A. Tegos, D. Tyrovolas, P. D. Diamantoulakis, C. K. Liaskos and G. K. Karagiannidis, "On the Distribution of the Sum of Double-Nakagami Random Vectors and Application in Randomly Reconfigurable Surfaces," IEEE Transactions on Vehicular Technology, vol. 71, no. 7, pp. 7297-7307, July. 2022.
- [66] P. S. Bouzinis, N. A. Mitsiou, P. D. Diamantoulakis, D. Tyrovolas and G. K. Karagiannidis, "Intelligent Over-the-Air Computing Environment," IEEE Wireless Communications Letters, vol. 12, no. 1, pp. 134-137, Jan. 2023.
- [67] B. Zhang, K. Yang, K. Wang and G. Zhang, "Performance Analysis of RIS-Assisted Wireless Communications with Energy Harvesting," IEEE Transactions on Vehicular Technology, vol. 72, no. 1, pp. 1325-1330, Jan. 2023.
- [68] C. Zhang, Y. Huang, C. He, C. Pan and K. Wang, "Energy Optimization for IRS-Aided SWIPT under Imperfect Cascaded Channels," IEEE Transactions on Vehicular Technology, pp. 1-13, Apr. 2023.
- [69] Anas Alkhatieb, Khaled Rabie, Xingwang Li, Galymzhan Naurzybayev, Ramez Alkhatib, "IRS-aided UAV for Future Wireless Communications: A Survey and Research Opportunities", arXiv:2212.06015, Dec. 2022.



Yangzhe Liao received his B.S. degree in Measurement and Control Technology from Northeastern University, China in 2013 and Ph.D. degree from the University of Warwick, UK, in 2017. Currently, he is an associate professor at the School of Information Engineering, Wuhan University of Technology, China. His research interests include mobile edge computing and mobile computing.



Jiaying Liu obtained her BS degree from the Wuhan University of Technology, China in 2020. Currently, she is pursuing her master's degree at the School of Information Engineering, Wuhan University of Technology, China. Her research interests mainly focus on wireless resource allocation and networking.



Gabriel-Miro Muntean (F'23) is a Professor with the School of Electronic Engineering, Dublin City University (DCU), Ireland, and co-Director of the DCU Performance Engineering Laboratory. He has published over 500 papers in top-level international journals and conferences, has authored 4 books and 28 book chapters, and has edited 6 additional books. He has supervised to completion 26 PhD students and has mentored 20 post-doctoral researchers and fellows. His research interests include quality, performance, and energy saving issues related to rich media content delivery, technology enhanced learning, and other data communications over heterogeneous networks. He is an Associate Editor of the IEEE TRANSACTIONS ON BROADCASTING, Multimedia Communications Area Editor of the IEEE COMMUNICATIONS SURVEYS AND TUTORIALS, and chair and reviewer for important international journals, conferences, and funding agencies. He was Project Coordinator and DCU Partner leader for the EU projects NEWTON and TRACTION.



Xiyu Chen is currently pursuing the master's degree in communication engineering with the School of Information Engineering, Wuhan University of Technology, China. Her research interests include resource allocation in wireless communications and network optimization.



Yi Han received the B.Eng. degree from the International School of Software, Wuhan University, China, in 2010, and the M.S. degree in telecommunication from Dublin City University, Ireland in 2011. He then obtained the Ph.D. degree from the Performance Engineering Laboratory, University College Dublin, Ireland. He is currently an associate professor with the School of Information Engineering, Wuhan University of Technology, China. His research interests include QoE assessment and performance-aware adaptive multimedia delivery.



Qingsong Ai received his M.S. and Ph.D. degrees from Wuhan University of Technology, China, in 2006 and 2008, respectively. From 2006 to 2007, he was a visiting researcher at the University of Auckland, New Zealand. He is currently a full Professor at the Wuhan University of Technology and Hubei university, China. Prof. Ai is the project leader of 12 national, ministerial or provincial projects with the total amount of 13M RMB. He has published over 70 international journal papers. His research interests include signal processing, rehabilitation robots and manufacturing technology.

manufacturing technology.